The Future Exploration of Saturn

By Kevin H. Baines, Sushil K. Atreya, Frank Crary, Scott G. Edgington, Thomas K. Greathouse, Henrik Melin, Olivier Mousis, Glenn S. Orton, Thomas R. Spilker, Anthony Wesley (2019). pp 417-441, in *Saturn in the 21st Century* (eds. KH Baines, FM Flasar, N Krupp, T Stallard), Cambridge University Press. https://doi.org/10.1017/9781316227220.014

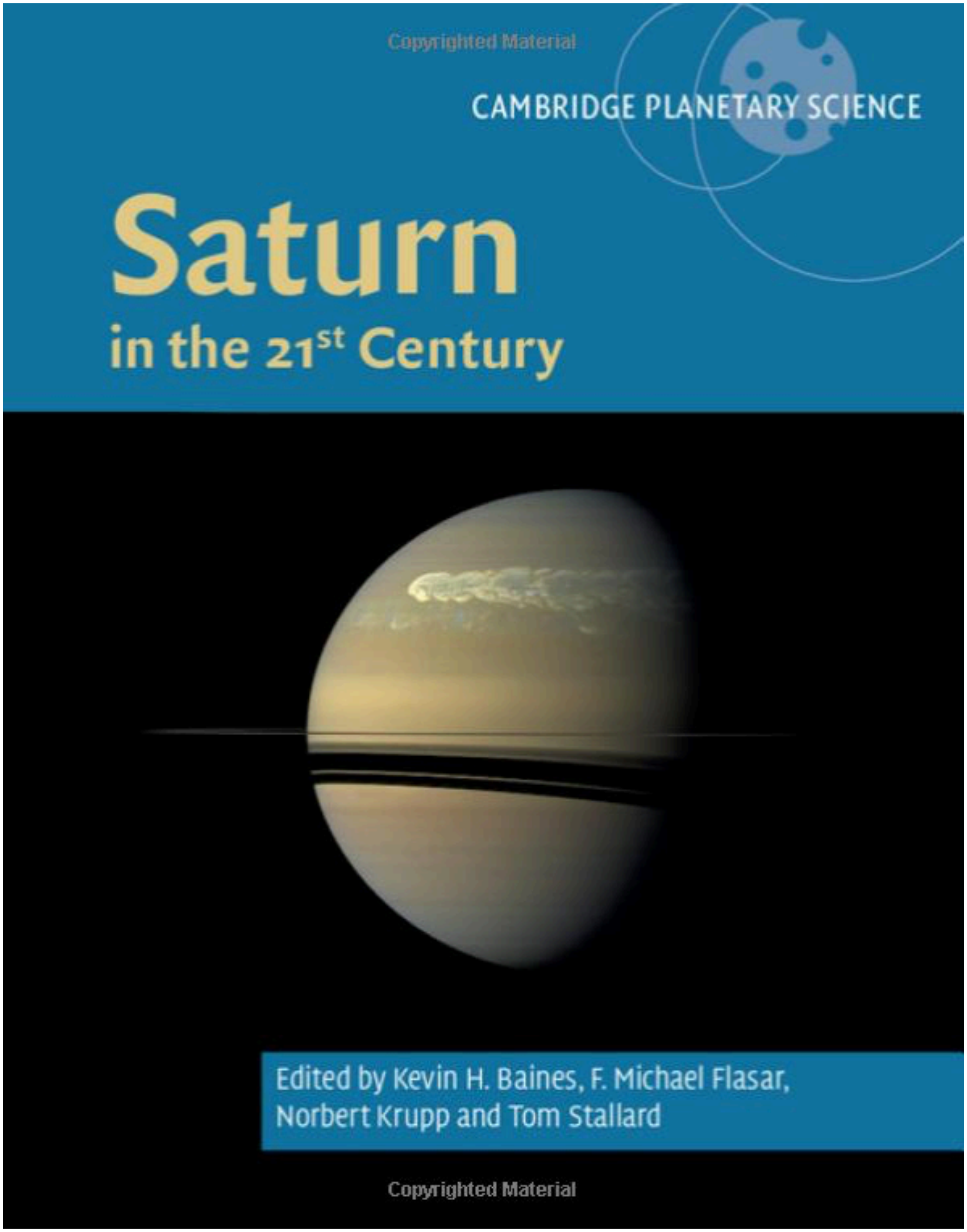

14

The Future Exploration of Saturn

KEVIN H. BAINES, SUSHIL K. ATREYA, FRANK CRARY, SCOTT G. EDGINGTON, THOMAS K. GREATHOUSE, HENRIK MELIN, OLIVIER MOUSIS, GLENN S. ORTON, THOMAS R. SPILKER AND ANTHONY WESLEY

Abstract

Despite the lack of another Flagship-class mission such as Cassini–Huygens, prospects for the future exploration of Saturn are nevertheless encouraging. Both NASA and the European Space Agency (ESA) are exploring the possibilities of focused interplanetary missions (1) to drop one or more in situ atmospheric entry probes into Saturn and (2) to explore the satellites Titan and Enceladus, which would provide opportunities for both in situ investigations of Saturn's magnetosphere and detailed remote-sensing observations of Saturn's atmosphere. Additionally, a new generation of powerful Earth-based and near-Earth telescopes with advanced instrumentation spanning the ultraviolet to the far-infrared promise to provide systematic observations of Saturn's seasonally changing composition and thermal structure, cloud structures and wind fields. Finally, new advances in amateur telescopic observations brought on largely by the availability of low-cost, powerful computers, low-noise, large-format cameras, and attendant sophisticated software promise to provide regular, longterm observations of Saturn in remarkable detail.

14.1 Introduction

Since the first planetary flyby in 1962, planetary exploration via spacecraft has proven time and again to be the most effective means to expand our knowledge of the Solar System. The Cassini/Huygens mission is arguably one of the most successful of such missions, achieving a remarkable record of discoveries about the entire Saturn system, including its icy satellites, the large atmosphere-enshrouded moon Titan, the planet's surprisingly intricate ring system and the planet's complex magnetosphere, atmosphere and interior. Far from being a small (500 km diameter) geologically dead moon, Enceladus proved to be exceptionally active, erupting with numerous geysers that spew liquid water vapor and ice grains into space – some of which falls back to form nearly pure white snowfields and some of which escapes to form a distinctive ring around Saturn (e.g. Spencer et al. 2009). Titan revealed itself to be an eerily Earthlike satellite covered with dozens of liquid hydrocarbon lakes and landscapes carved by river channels, both of which are linked to a complex methane-based meteorology complete with transient storm clouds that rain down from a nitrogen-based, smoggy sky some ten times thicker than that of Earth (e.g. Aharonson et al. 2014; Griffith et al. 2014). Similarly, Saturn's resplendent system of planet-girdling rings has revealed itself as host to a surprising number of organized and evolving features such as spiral waves – some of which may have been generated by slight gravitational perturbations within Saturn's interior (e.g. Chapter 3 by Fortney et al.; Chapter 5 by Carbary et al.) – and mysterious elongated clumps known as "propellers" that hint at processes analogous to the formation of solar systems around our Sun and other stars (e.g. Colwell et al., 2009).

Saturn itself has revealed that its typically serene, unperturbed appearance masks an underlying reality. At the poles, flickering aurorae constantly change shape and intensity, perhaps in response to variations

. https://doi.org/10.1017/9781316227220.014

in the solar wind brought on by solar storms, possibly augmented by the effects of Enceladus's geysers and ring rain (cf. Chapter 7 by Stallard et al.; Chapter 8 by Moore et al.). The north pole is capped by a mysterious, long-lived hexagonal feature bordering a polar vortex (cf. Chapter 12 by Sayanagi et al.). Underneath Saturn's upper skin of planet-girdling hazes, a surprising array of dynamical processes roil at depth. As detailed in Chapter 13 by Sánchez-Lavega et al., periodically – every three decades or so – a surprisingly powerful storm erupts, whose spreading clouds encircle the planet in a ~10°-wide latitudinal band centered on the storm. Indeed, the major storm of 2010–2011 well witnessed by Cassini and Earth-based observers has proved to be the most powerful convective storm system observed thus far on any planet, lofting materials over 150 km in altitude (e.g. Fletcher et al. 2011; Sanz-Requena et al. 2012; Sromovsky et al. 2013; Li and Ingersoll 2015).

The end of the Cassini-Huygens Mission in September 2017 concludes a remarkable thirteen-year era of exploration and discovery of Saturn, its moons, ring system and magnetosphere. For the foreseeable future, no comparable comprehensive orbital reconnaissance of the Saturn system is planned by any of the world's space agencies. Thus, it is unclear when the next concerted effort to explore the entire Saturn system via interplanetary spacecraft will be undertaken. In this chapter we detail the major science objectives for the future exploration of Saturn and the prime observational techniques that will likely be used over the next several decades.

14.2 Outstanding Science Issues

Here, we first review the science goals of the Grand Finale phase which concludes the Cassini Mission. Next we discuss scientific priorities for future Saturn research as defined by the Planetary Science Decadal Survey (PSDS) Committee, established by the National Research Council, in the PSDS 2011 Visions and Voyages report (NRC 2011). This document is of particular importance as it has been adopted by NASA's Science Mission Directorate as the primary guiding document for the Directorate's strategic planning of planetary exploration for the current decadal period of 2013–2023. In our discussion, we provide additional details on the major science priorities, especially regarding the need to make measurements diagnostic of the planet's origin and evolution.

14.2.1 Priority Science Goals of the Cassini Grand Finale Mission

In orbit since 1 July 2004, the Cassini Orbiter began its final phase of science investigations in December, 2016. Entitled the Grand Finale – as it concludes with a 34-km s^{-1} plunge into Saturn on 15 September 2017 – the Cassini Orbiter will spend its final five months circling the planet in a highly elliptical, highly inclined orbit, diving 22 times inside the innermost rings to fly swiftly (> 36 km s^{-1}) past the planet just ~2000 km above its equatorial cloud tops (Figure 14.1). These novel orbits are achieved by a gravitational kick from Titan in April 2017 that jumps the spacecraft's periapsis (i.e. the closest point to Saturn's center) from just outside Saturn's main rings, some 87,000 km above the cloud tops, into the clear gap between the innermost D ring and the upper atmosphere. The unique observational geometry allows Cassini to gather unprecedented close-up views of the planet and its rings, while also obtaining in situ samples of gases, dust, plasma and

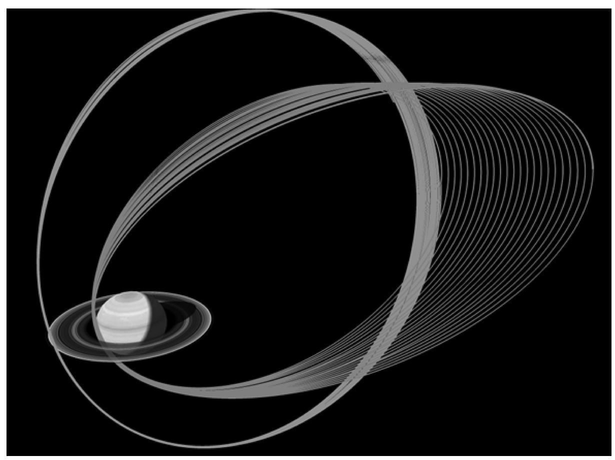

Figure 14.1 The final ten months of the Cassini–Huygens Mission to Saturn: F Ring and Grand Finale Orbit phase. Twenty orbits just outside the F Ring (grey) transition to twenty-two Grand Finale Orbits (blue) between Saturn and its innermost rings and the planet, when the orbital periapsis drops to ~3,000 km above Saturn's cloud tops, vs ~200,000 km during previous closest approaches. The last half-orbit (orange) plunges Cassini into the atmosphere of Saturn (image courtesy of NASA/JPL-Caltech). (A black-and-white version of this figure appears in some formats. For the color version, please refer to the plate section.)

magnetic fields. Altogether, the unique data collected during the Grand Finale phase addresses key issues about Saturn, its rings and its innermost plasma environment, similar to those being addressed by the Juno mission at Jupiter, thus promising new synergistic insights into how each planet formed, evolved and works today.

Salient Grand Finale science measurement objectives, as are only obtainable by such close-up passes, include (1) the first measurements of the higher-order gravitational and magnetic field moments to constrain Saturn's interior structure and possibly determine its currently unknown internal rotation rate; (2) in situ measurements of Saturn's ionosphere, innermost radiation belts, dust environment and auroral acceleration region; (3) accurate measurement of main ring mass, currently uncertain by about an order of magnitude; (4) high-spatial-resolution studies of the main rings, including novel probing by radar; and (5) high-spatial-resolution Saturn atmospheric observations and in situ sampling of outflowing ions. With an orbital periapse near local solar noon and slightly south of the ring plane, Cassini will be well placed to obtain optimized gravity measurements and high-resolution imaging and occultation measurements of the main rings. Cassini will approach the periapse over the northern hemisphere for inbound observations of the sunlit rings and Saturn's north polar regions, including the long-lived polar hexagon feature (see Chapter 12). Outbound trajectories will provide excellent views of southern aurora and the south pole in winter, as well as the unlit side of the rings.

14.2.1.1 Interior and Magnetic and Gravitational Fields

During the Grand Finale, Cassini's magnetometer will measure the magnetic field as close as 1.03 Saturn radii from Saturn's center to derive high-order coefficients to degree-9 and possibly degree-11, which then will determine the depth of Saturn's metallic hydrogen core, important for understanding the dynamo mechanism in the deep interior. Furthermore, as discussed in Section 14.2.4, these close-up measurements are Cassini's best chance for characterizing any asymmetry in the magnetic field, which will not only help to characterize the planet's dynamo but may finally determine the bulk rotation rate of the planet, perhaps to better than ±0.1%. Existing data show some statistical evidence of asymmetries at the 20 nT-R_S^3 level (Burton and Dougherty 2014), implying a small ~0.05° tilt, thus making direct measurements challenging.

The low-order harmonics of the gravity field give information about the mass of the core and possible internal layering, while the high-order harmonics are diagnostic of the winds in the deep interior. Radio science data from a number of dedicated gravity passes will determine the zonal gravity harmonics up to degree-12 (J_{12}) with an error of less than 2×10^{-7} – at least two orders of magnitude better than current values for J_{10}. This will provide a determination of the vertical extent of the observed upper-level winds and may also reveal clues about the planet's rotation rate. In addition, Cassini may be able to measure the relativistic Lense–Thirring frame-dragging effect (Helled 2011), which would determine the planet's angular momentum and further constrain the rotation rate.

14.2.1.2 Atmosphere and Exosphere In Situ Sampling

For the first time, Cassini's ion and neutral mass spectrometer will sample in situ the neutral and ion composition and density of Saturn's ionosphere and thermosphere down to approximately the ~1000 km level above the clouds during the last five orbits of the mission. Composed mostly of molecular and atomic hydrogen and helium along with trace amounts of hydrocarbons and oxygen-bearing molecules, the directly measured inventory of both atomic and molecular species will provide new insights into the energetics and dynamics of the thermosphere, as well as provide a valuable constraint on the ever-elusive abundance of helium in the deep interior. Ionospheric structure will be investigated with in situ measurements of electron density and temperature by a Langmuir probe.

Flying interior to the D ring, Cassini will characterize the enhanced radiation environment that exists in the gap between the D ring and the upper atmosphere, a region never explored in situ. Cassini's dust analyzer will determine the composition and abundance of the so-called "ring rain" material that precipitates into the planet from the rings along magnetic field lines (cf. Chapter 8). Finally, these orbits will also provide a unique opportunity for studying the properties of lightning by searching for their characteristic whistler radio waves.

Cassini's Grand Finale phase thus amounts to a brand-new mission that is quite distinct in science and measurement objectives assigned heretofore to the Cassini Mission. Overall, Cassini sets the stage for future missions, leaving an incredibly rich legacy of discoveries that have changed our views of the Saturn system, how solar systems form from proto-planetary disks, and the potential for life elsewhere in our universe.

14.2.2 The 2011 Decadal Survey: Saturn Science and Exploration Goals

To establish priorities in NASA's planetary exploration program for the decade of 2013 to 2023, the Committee on the Planetary Science Decadal Survey (hereafter, the Decadal Committee), led by the National Research Council, was formed in 2009. Over 75 scientists and engineers were involved as committee members; several hundred other scientists participated in developing and submitting 199 white papers for committee consideration.

In their final report (NRC 2011), the Decadal Committee recommended that a Saturn Probe mission be included in the list of five candidate missions for the next New Frontiers competition, formally known as New Frontiers Mission 4. Key mission science objectives, similar to those promoted by ESA's Cosmic Vision Program (cf. Section 14.3.2.2), are to (1) determine the noble gas abundances and isotopic ratios of hydrogen, carbon, nitrogen and oxygen in Saturn's atmosphere, and to (2) determine the atmospheric structure including dynamics at the probe site.

The Decadal Committee found that the Saturn probe concept directly addresses two of its major themes (NRC 2011): (1) building new worlds and (2) understanding the workings of solar systems. In particular, the mission would directly address three of the committee's ten priority questions. Under the "building" theme, the mission would address the key questions of "How did the giant planets and their satellite systems accrete?" and "Is there evidence that they migrated to new orbital positions?" Under the "workings" theme, the mission addresses two priority questions: (1) "How do the giant planets serve as laboratories to understand the Earth, the solar system and extrasolar planetary systems?" and (2) "How have the myriad chemical and physical processes that shaped the solar system operated, interacted and evolved over time?"

14.2.2.1 Building New Worlds: Clues from Elemental Abundances

Perhaps the highest priority question for Saturn pertains to its origin and overall history: *How did Saturn form and evolve?* A prime mystery linking Saturn to the primordial past is why the planet emits more than twice the energy it absorbs from the Sun, indicating a large source of internal heat associated with its origin and evolution over the æons.

The observed heavy element enrichment in Jupiter (via Galileo probe; Niemann et al. 1998) and Saturn (carbon from Cassini spectral observations of methane; Fletcher et al. 2009a) and the frequency and characteristics of exoplanets provide overwhelming evidence in favor of the core accretion model for Saturn's formation (for a detailed discussion, see Chapter 2 by Atreya et al.). It is generally accepted that Saturn's core formed from heavy elements (mass > ^{4}He), originally delivered in water ice. Although the composition of Saturn's core cannot be studied directly, being 40,000–50,000 km below Saturn's visible clouds, key core-forming heavy elements are released from the core during accretionary heating and mixed to the upper troposphere, where they can be measured. A comparison of the abundances of Saturn's heavy elements and their isotopes with those in the Sun and the other gas giant planet, Jupiter, would then provide the set of essential constraints needed to develop accurate models of the formation and evolution of Saturn and the other giant planets.

As discussed in Chapter 2 by Atreya et al., carbon – as determined from remote-sensing measurements of well-mixed methane gas in Saturn's visible atmosphere – is the only heavy element in Saturn whose abundance is determined precisely, with a C:H ratio nine times solar (Table 2.1). Due to the inability of remote sensing instruments to probe condensable volatiles such as ammonia, hydrogen sulfide and water below their respective clouds, reliable measurements of Saturn's bulk N:H, S:H and O:H are lacking. Similarly, the P:H ratio is determined precisely from PH_3 in the upper

. https://doi.org/10.1017/9781316227220.014

troposphere, but due to the possible loss and fractionation of PH_3 in convective upwelling from its thermochemical equilibrium level at ~1000 bar to the upper atmosphere, such P:H upper tropospheric measurements may not be indicative of the value in the deep atmosphere. As well, the noble gases cannot be measured by remote sensing. For distinguishing between Saturn formation models, it is essential to determine the abundances of all of the noble gases and their isotopic ratios, together with the abundances of C, N, S and O, and the isotopic ratios, D:H in H_2, ^{13}C:^{12}C in CH_4, ^{15}N:^{14}N in NH_3, ^{34}S:^{32}S in H_2S and ^{18}O:^{16}O in H_2O (cf. Chapter 2).

Entry probes at relatively shallow depths (~10 bar) can measure the elemental abundances and isotopes of the nobles, and N and S. However, the accurate measurement of the oxygen abundance derived from its primary reservoir, condensable water, requires that probe measurements be made at depths well below the 10–20-bar water condensation level, that is, at 50–100 bar (cf. Figure 2.9 and associated discussion in Chapter 2). However, water in Saturn's deep atmosphere can also be measured by passive microwave radiometry from Saturn orbit, as at Jupiter by the Juno mission. Including this technique, entry probes sampling down to the 10-bar level would be sufficient.

Direct in situ measurement of Saturn's helium abundance yields additional constraints on the models of Saturn's formation, interior and the heat budget. As discussed in Chapter 2, Saturn's He:H ratio is highly uncertain, with a current best estimate of 0.58–0.84 of the solar ratio (Table 2.1). The depletion of helium relative to the Sun measured in the upper troposphere of Jupiter is attributed to the condensation of helium gas into liquid helium at the 1–2 megabar level in the planet's interior. If the current He:H estimate at Saturn is confirmed, it would imply that the condensation of helium also occurs in Saturn's interior, as currently predicted by interior models (see Chapter 3 by Fortney et al. and references therein). The condensation of helium and subsequent differentiation of helium droplets from hydrogen in the planet's interior would release both latent heat and gravitational potential energy, which contribute to the planet's thermal evolution, anomalously high temperature, and energy balance (see Chapter 2).

14.2.2.2 Building New Worlds: Understanding Saturn's Rotation Rate

As discussed in Chapter 5 by Carbary et al., a surprisingly large uncertainty currently surrounds Saturn's rotation rate. If attempts to measure Saturn's bulk rate of rotation from magnetic field measurements during Cassini's Grand Finale (cf. Section 14.2.1.1) fail, the answer may ultimately be determined through Earth-based observations of Saturn's rings. Near equinox, Earth crosses Saturn's ring plane. Nicholson et al. (1999) noted that the observed timing of these crossings can be used to determine the direction of Saturn's spin axis and the precession rate of the pole, which yields constraints on the planet's angular momentum. Given constraints on the planet's moment of inertia from Cassini's close-up gravity measurements during the Grand Finale, ring-plane-crossing observations should, eventually, accurately determine the rotational period. With only two sets of observations possible per Saturn year (6–7 per century) the required data may take many decades to acquire, but this approach may finally definitively determine Saturn's rotation rate.

14.2.2.3 Understanding the Workings of Solar Systems: Saturn's Atmospheric Variability, Seasonal and Otherwise

Saturn displays a wide range of atmospheric phenomena that vary over a large variety of time scales. These phenomena include changes in temperature, composition and cloud properties (cf. Chapter 10 by Fletcher et al.). Long-term changes that take place on the order of thirty years are likely largely driven by the seasonal variation of sunlight, modified by the nonlinear dynamical and thermodynamic response of the atmosphere. Shorter-term changes may be driven by seasonal forcing or could be completely uncorrelated with seasonal changes. Cassini and ground-based observations have identified seasonal trends in temperature (Chapter 10) as well as events that seem at first glance isolated in time, e.g. the Great Storm of 2010–2011 (cf. Fischer et al. 2011; Chapter 13 by Sánchez-Lavega et al.). It is clear that the atmosphere is driven by more long-term influences than merely seasonal changes of incident sunlight. For example, dynamical features, such as the long-lived (> 1 Saturn year) polar hexagon (cf. Chapter 12 by Sayanagi et al.) and the "string of pearls"

(Chapter 13), along with episodic (~30 years) great storms appear to be confined to the northern hemisphere (cf. Figure 14.6 and Chapter 13), while "storm alley" (cf. Figure 14.5 and Chapter 11 by Showman et al.) seems to be confined to the southern hemisphere near 35° south latitude. What, exactly, are the timescales – seasonal or non-seasonal – of such hemispherically asymmetric features and what are their drivers? Zonal thermal waves also appear to differ significantly in the northern and southern hemispheres during the ~40% of a Saturn year observed by Cassini, but this is too short a time to clearly establish the seasonality of atmospheric phenomena. Therefore, it is left to future ground-based and space-based observations to identify and characterize the full range of phenomena that are distinctly the result of seasonal changes of insolation. As detailed in Section 14.4.1, characterizing these changes will include combinations of observations at all wavelengths and at high-spatial and high-spectral resolution, by both state-of-the-art ground and space-based platforms.

14.2.2.4 Understanding the Workings of Solar Systems: Saturn's Magnetospheric Interactions and Aurorae

Significant gaps in our understanding of Saturn's auroral processes exist (cf. Chapter 7 by Stallard et al). The variable rotating phenomenon, known as the planetary period oscillation is a major outstanding issue. Found at thermospheric/stratospheric altitudes by Cassini, they occur at different rates in the northern and southern hemispheres. From Earth, this phenomenon had been previously positively identified in HST ultraviolet auroral observations (Nichols et al. 2010). Auroral radio emissions are observable by spacecraft located many AU from Saturn (Lecacheux and Aubier 1997), but not from the Earth's surface, as these emissions are below the ionospheric plasma cutoff frequency of ~5 Mhz. Apart from equinox, Earth-based platforms see only a single pole. This renders the characterization of the two periodicities impossible after Cassini's 2017 end until at least the 2024 equinox. However, if the ultimate source of the periodicities rests within the atmosphere (e.g. Smith 2006; Jia and Kivelson 2012; Southwood and Cowley 2014), then the thermospheric or upper stratospheric vortices may be observable to ground-based telescopes equipped with high-spectral-resolution infrared spectrographs and adaptive optics (AO).

Voyager found that the global upper atmosphere is much hotter than predicted by current models (e.g. Müller-Wodarg et al. 2012). Although auroral processes are capable of injecting significant energy into the uppermost reaches of the atmosphere, it remains unclear how this energy could be redistributed to lower regions. The Cassini mission has provided a number of important constraints on ionospheric and thermospheric phenomena via, for example, multiple UV stellar occultations (Koskinen et al. 2013) and Cassini/VIMS H_3^+-derived temperature measurements (Stallard et al. 2012). Similar ground-based observations of H_3^+ emissions as well as ring-rain (O'Donoghue et al. 2013) will continue post Cassini, providing new insights into how energy is injected at low latitudes, how this interaction evolves as the ionosphere changes with season, and thus overall how the mechanisms that govern the energy balance of Saturn's upper atmosphere operate.

14.3 Future Saturn Missions

The remarkable record of surprising discoveries from the Cassini-Huygens mission has given rise to a plethora of new science issues as well as reinforced the quest to obtain long-sought-after measurements, such as the planet's unknown composition at depth. Thus, the scientific community and chief governing space agencies, NASA and ESA, have been spurred to investigate possible future missions to the Saturn system. NASA studies have included both large ~$2 billion Flagship missions and more modest (~$1 billion) New Frontiers Missions for potential flights in the 2020s. In Europe, several missions have been proposed to ESA's Cosmic Visions opportunities for flight in the 2020s and 2030s. All such missions must contend with the relatively complex nature of travel to and operations at Saturn, as we now explore.

14.3.1 Issues Common to Saturn Missions

Prime issues dictating the cost and complexity of Saturn missions are (1) the time-of-flight and energy needed to rendezvous with a planet 9.5 AU from the Sun, (2) the data rate achievable from that distance and

. https://doi.org/10.1017/9781316227220.014

(3) the means to maintain operational systems, including the generation of adequate electric power. Perhaps the most challenging issue is how to reliably fly to Saturn within viable constraints of cost and travel time, which fundamentally depends on spacecraft mass. Beyond the mass of the science payload and associated reliable systems for operations, for orbiter missions the additional mass of the fuel required for velocity adjustments to visit other Saturn system targets such as moons and rings can amount to a significant fraction of the total vehicle mass.

Travel to Saturn involves a change in gravitational potential energy of approximately 8×10^8 J per kg of transferred mass, roughly the chemical energy available from 100 1-kg sticks of dynamite. This energy has been typically supplied by some combination of propulsion (chemical rocket engines, electric propulsion engines, etc.) and gravity assist by intervening planets (e.g. Zander 1964; Doody 2004). Future missions might use more exotic forms of propulsion such as solar sails.

The availability of multiple means for accelerating spacecraft results in a wide variety of Earth-to-Saturn trajectories of varying complexity. Simpler trajectories rely on the launch vehicle and post-launch active propulsion for most of the transfer energy. Some of these are similar to the classical Hohmann transfer (Hohmann 1925), an energy-efficient transit that utilizes an eccentric orbit to connect a pair of concentric circular, coplanar orbits at two tangent points. However, the orbits of Earth and Saturn are neither exactly circular nor coplanar; thus, trajectories that accommodate these "quasi-Hohmann" transfers require somewhat more energy. All of these direct trajectories require at least a six-year cruise and a relatively large amount of energy, resulting in large launch vehicle costs. No Saturn mission has used a direct Earth-to-Saturn transfer, testimony to the effectiveness of using gravity assists (GA) instead of rocket engines to provide a significant fraction of the required energy.

Jupiter's large mass renders it an efficient GA engine for reaching Saturn. Pioneers 10 and 11 and both Voyagers used Jupiter gravity assists (JGA) to reach Saturn and beyond, saving about 25% of the direct Earth-to-Saturn transfer energy. This also decreased the trip time with respect to the direct trajectory: Voyager 1 traveled to Saturn in slightly less than 3.2 years. The main disadvantage of JGAs is the long, ~20-year interval between the openings of relatively short ~2-year usable windows. The Voyagers, launched in 1977, utilized the 1979–1980 Jupiter window, while the Cassini-Huygens mission, launched in 1997, used the 1999–2000 window. With no missions making use of the 2018–2020 window, 2038 is the next opportunity for an efficient JGA push to Saturn.

Significant launch energy can be saved through the use of additional planetary GA pushes and/or the use of solar electric propulsion (Lam et al. 2009). One fruitful strategy, as employed by both Galileo and Cassini, is to conduct multiple encounters of terrestrial planets to reach Jupiter. In particular, Cassini used two GAs at Venus and one at Earth, saving more than 80 of those 100 sticks of dynamite per kg of transferred mass.

The use of terrestrial planets for GA opens up more Saturn launch opportunities. Many such trajectories use combinations of Venus, Earth and even Mars GAs, and some are ballistic, meaning they do not need pre-planned propulsive maneuvers. Another technique uses an Earth GA (EGA) without a flyby of Venus or Mars, but instead requires a propulsive deep space maneuver (DSM) before the EGA, hence the designation "ΔVEGA," where "ΔV" denotes a change in velocity provided by the DSM (Doody 2004). This technique offers more flexible schedules since opportunities occur every Earth-Saturn synodic period, ~1.034 years, but they require significantly larger propulsion when Saturn is far out of Earth's ecliptic plane at arrival. However, solar electric propulsion may render this a viable option.

14.3.2 Saturn Mission Studies

Armed with such trajectory strategies, NASA and ESA have explored a number of potential post-Cassini Saturn missions, focusing on (1) key aspects of unachieved Saturn measurements – such as the abundances of noble gases and their isotopes and the composition of volatiles such as ammonia and water at depth – and (2) answering fundamental new questions arising from the Cassini discoveries. Both NASA and ESA studies have focused on using a descent probe for direct sampling of atmospheric constituents and measurements of winds, particularly in the unexplored region below the upper tropospheric cloud layers.

Figure 14.2 The ESA-proposed M5 Hera Saturn entry probe descending under parachute through the Saturn skies. Having safely delivered the probe through atmospheric entry, the conical heat shield is seen falling away, enabling atmospheric sampling to begin. From Mousis et al. (2016). Artwork by T. Balint. (A black-and-white version of this figure appears in some formats. For the color version, please refer to the plate section.)

Figure 14.2, from the ESA 2016 Hera M5 proposal (Mousis et al. 2016; Section 14.3.2.2) depicts the descent of such an entry probe on parachute just after release of its conic heatshield.

14.3.2.1 NASA Saturn Mission Studies

The Decadal Committee developed and evaluated the viability of two Saturn system mission concepts, with a key objective of keeping total mission cost below ~$2 billion in 2012 dollars. These were (1) a Titan-oriented mission concept that built on the NASA 2009 Flagship-class "Titan Saturn System Mission" (TSSM) mission study (NASA/ESA 2009; Reh et al. 2009), and (2) a New Frontiers class entry probe mission to explore, in situ, Saturn's atmosphere.

14.3.2.1.1 Titan Saturn System Mission (TSSM)

The 2009 Flagship-class TSSM concept included (1) a Titan orbiter that would visit Enceladus en route to entering Titan orbit, and (2) two probe elements for exploring Titan in situ – a Montgolfière hot-air balloon and a lander that would set down on a hydrocarbon lake. Utilizing remote-sensing and mass spectrometers on all three platforms, the mission would spectrally map and sample the gases and aerosols of both Titan and Enceladus, as well as study the magnetosphere and atmosphere of Saturn, including in-depth scrutiny of Saturn's storms and other meteorological features. However, the Decadal Committee estimated that TSSM cost exceeded the $2 billion budget, and thus judged TSSM non-viable for the 2013–2022 period.

14.3.2.1.2 The New Frontiers Class Saturn Probe Mission

The Decadal Committee established the mission science objectives for a New Frontiers class Saturn probe (SP) mission, as outlined in Section 14.2.2, and studied a number of SP mission concepts to determine their viability. For these studies, only the most important objectives – known as Tier 1 – were addressed.

The resulting SP mission concept resembles a simpler version of the Jupiter Galileo orbiter/probe mission. The flight system consists of a probe and a flyby carrier-relay spacecraft (CRSC) that would both deliver the probe to an entry trajectory and relay the probe data to Earth. The probe would enter Saturn's atmosphere at a velocity of 26–30 km s^{-1}, significantly less than the 47.4 km s^{-1} experienced by the Galileo probe. After the entry heating and deceleration period, the probe's aeroshell would be jettisoned near the 0.1-bar pressure level, allowing the probe to commence in situ science experiments and data transmission. The descent module would descend to the 5-bar level some 55 minutes later and 210 km below where transmissions began. (Descending to the 10-bar level is preferred, but is challenging, as noted below.) Throughout the descent, the CRSC's antenna would continuously point at the entry site, recording and relaying to Earth about 2 Mb of data, some 3 times that returned by the Galileo probe.

The main conclusions of this SP mission study were

1. Such a mission can fit into the New Frontiers Program resource constraints.
2. Solar power is a feasible option.

3. The cost difference between solar and nuclear power systems is relatively small.
4. A mid-sized launcher can deliver a flight system to Saturn without a Jupiter GA in an acceptable time frame.
5. No new technologies are needed.

Conclusion 3 assumes that the Advanced Stirling Radioisotope Generator (ASRG) would be available at the NASA-stated cost. However, NASA has since cancelled the ASRG development program. The alternative nuclear electric source, the Multi-Mission Radioisotope Thermoelectric Generator (MMRTG), is more massive and expensive, so that trade must be revisited. Conclusion 4 stems from the finding that the flight system and trajectory easily fit the relatively small Atlas 401. However, a launch at a time when Saturn arrival is far out of Earth's ecliptic plane might require the next larger launcher. Conclusion 5 stems from the ongoing development of NASA's Heat-shield for Extreme Entry Environment Technology (HEEET) task for use at Saturn. NASA plans for this technology to be available at Technology Readiness Level (TRL) 6, appropriate for competed mission proposals, by late 2017.

The study also produced a noteworthy technical result concerning descent profiles. Due to Saturn's larger atmospheric scale height and weaker gravitational acceleration, a descent under a single Galileo-like parachute for the entire desired 10-bar descent exceeds the duration of the 60- to 90-minute data-relay window provided by the CRSC overflight. However, a reduction in parachute size for faster descents results in an inadequate vertical sampling rate. Possible options include (1) deployment of a parachute sized for the slower descent through the upper levels, then at a pre-determined pressure level reefing or releasing the parachute to continue the remaining descent in free-fall, or (2) following the Huygens–Titan probe design, deployment of a smaller parachute after the first is released.

The Saturn probe study suggests that such a mission is a feasible candidate for NASA's New Frontiers Program (NFP). Indeed, NASA has added a Saturn probe mission to NFP's list of desired missions for the 2016 Announcement of Opportunity, with Step 1 proposals due by May, 2017.

14.3.2.2 ESA Saturn Probe Mission Studies

Several Saturn probe concepts utilizing both simple carriers and more complex orbiters have been submitted by European scientists and engineers to calls by the ESA Cosmic Vision Program. In recent years, three configurations of varying complexities have been considered (Coustenis et al. 2014; Mousis et al. 2014):

– Configuration 1 (Probe and Carrier). The least costly option, this concept specifies that the probe transmit its data via a direct-to-Earth (DTE) radio-frequency link. The carrier follows the probe into the atmosphere, perhaps performing pre-entry science observations which it would also transmit DTE prior to its atmospheric plunge.

– Configuration 2 (Probe and Carrier/Relay). This concept is similar to the New Frontiers Class concept discussed in Section 14.3.2.1.2, where the carrier relays probe data to Earth. The carrier would release the probe several weeks prior to entry, after which the carrier trajectory would be deflected for overflight phasing of the probe descent location to conduct both probe data relay and approach and flyby science.

– Configuration 3 (Probe and Orbiter). This configuration would be similar to the Flagship Class Galileo Orbiter/Probe mission. As with Configuration 2, the carrier would release the probe several months prior to probe entry and then subsequently deflect to prepare for overflight phasing of the probe descent location. After probe relay, the orbiter would go into Saturn orbit to conduct orbital science.

In all three configurations, solar panels would be used to provide electrical power for the carrier/orbiter, with batteries included for high power demand periods, such as during probe entry. Nuclear power would be considered for the carrier/orbiter only if solar power technology were not feasible. All configurations would allow the carrier/orbiter to perform several months of approach science. Configuration 1 allows in situ pre-entry science by the carrier. Configuration 2 would possibly provide flyby science, and would allow redundant retransmissions of the probe data. With its orbital capabilities, Configuration 3 would be both the most scientifically interesting and most expensive option. As detailed below, the Large-Mission-class Kronos Mission Concept developed in 2007 expanded on Configurations 2 and 3, calling for two probes. As discussed in Section 14.3.2.2.2, the 2015 Medium-Mission-class Hera concept called for a single probe and a relay carrier, adhering closely to Configuration 2.

14.3.2.2.1. The Kronos Mission Concept for ESA Cosmic Vision 2015–2025 The Kronos (Greek name for Saturn) mission (Marty et al. 2009) was submitted to the ESA Cosmic Vision call (ESA 2007) for large missions (900 million euros). The mission's aim was to perform (i) in situ measurements of the chemical and isotopic composition of Saturn's atmosphere via two ESA probes delivered by a single NASA carrier spacecraft and (ii) remote sensing from space by carrier spacecraft instruments to better understand the formation of Saturn and the origin of its atmosphere. The probes were designed to perform in situ measurements of Saturn's atmosphere down to a depth of about 10 bar. Compared to a carrier flyby option, an orbiter configuration would have enabled a more global investigation of Saturn's atmospheric H_2O and NH_3, the planet's gravity and internal magnetic fields, the ring system and the inner magnetosphere. However, the mission would have required additional propellant tanks and a modified power system to deliver higher power.

Because Kronos was proposed as an international collaboration between ESA and NASA, both US and European solutions were considered for the launch vehicle. The total mass of the two-probe flyby-based architecture was estimated at less than 3000 kg, implying that the launch vehicle for the mission could be an Atlas V-551 or equivalent. Chemical and/or solar electric propulsion systems were envisaged for the spacecraft, leading to trajectories with flight times ranging from ~6 to 17 years, with <12 year trajectories much preferred. For carrier power, Low Intensity Low Temperature (LILT) solar panels inherited from the Juno and Bepi Colombo missions were considered. To provide the least risky mission architecture possible, the probes were expected to use batteries and a DTE communication strategy, and to arrive at or near the sub-Earth point on Saturn. For ring science, the Kronos proposal also suggested that the carrier could drop off a fleet of two or three very small, identical probes directly into the rings, with each probe carrying a single efficient camera to acquire high-resolution ring images.

The proposed Kronos Saturn probes used significant heritage from the Galileo probe, including the Thermal Protection System (TPS) and aeroshell design. The Huygens Titan probe provided technological heritage for the operation of the descent modules deployed from the two Kronos atmospheric probes.

The two key Kronos probe instruments were a mass spectrometer (Saturn Probe Gas Analysis System; SPGAS) and an Atmospheric Structure Instrument (ASI). The proposed SPGAS quadrupole mass spectrometer was inherited from the successful Galileo Jupiter and Cassini/Huygens probe composition/isotope investigations (Niemann et al. 1998, 2005). Similar to the Cassini/Huygens ASI experiment (Fulchignoni et al. 2002), the Kronos ASI consisted of three primary sensor packages: (1) a three-axis accelerometer, (2) a pressure profile instrument and (3) temperature sensors. In addition, in the upper atmosphere, deceleration measurements provided the atmospheric density, pressure and temperature profiles prior to pressure/temperature sensor deployment.

Other envisaged probe instruments included a nephelometer to determine the aerosol number density, and the sizes, shapes and index of refraction of aerosols, and a Doppler Wind Experiment (DWE) – based on the successful Galileo and Huygens designs (e.g. Atkinson et al. 1998) – to measure the vertical profiles of the zonal (east-west) winds along the probe descent paths.

For the carrier, the payload science objectives were close to those of the Juno mission. In particular, key objectives were to secure the deep, global abundances of H_2O and NH_3, as well as their distributions over all latitudes, using microwave radiometry.

14.3.2.2.2 Recent ESA Probe Concepts: The Hera Mission

In 2010, ESA assessed Planetary Entry Probes (PEP) for Venus, Saturn, Uranus and Neptune (ESA 2010) for their feasibility to investigate these planets down to 100 bar (target)/30 bar (threshold). In this study, the designs of the four probes were similar in general layout, mass and payload (see Figure 14.3). In the case of Saturn, solutions were found allowing descent from ~1 to 100 bar in ~90 minutes.

Capitalizing on these results, in January 2015 a proposed mission entitled Hera – after the daughter of Kronos in Greek mythology – was submitted to the ESA call for medium-class missions (M4). This latest proposal followed the Configuration 2 concept discussed above, with a flyby telecom carrier and a single probe. Given the reduced cost of the M4 mission, this concept was less ambitious than the PEP Saturn concept, reaching a depth of just 10 bar, sufficient to measure the noble gases,

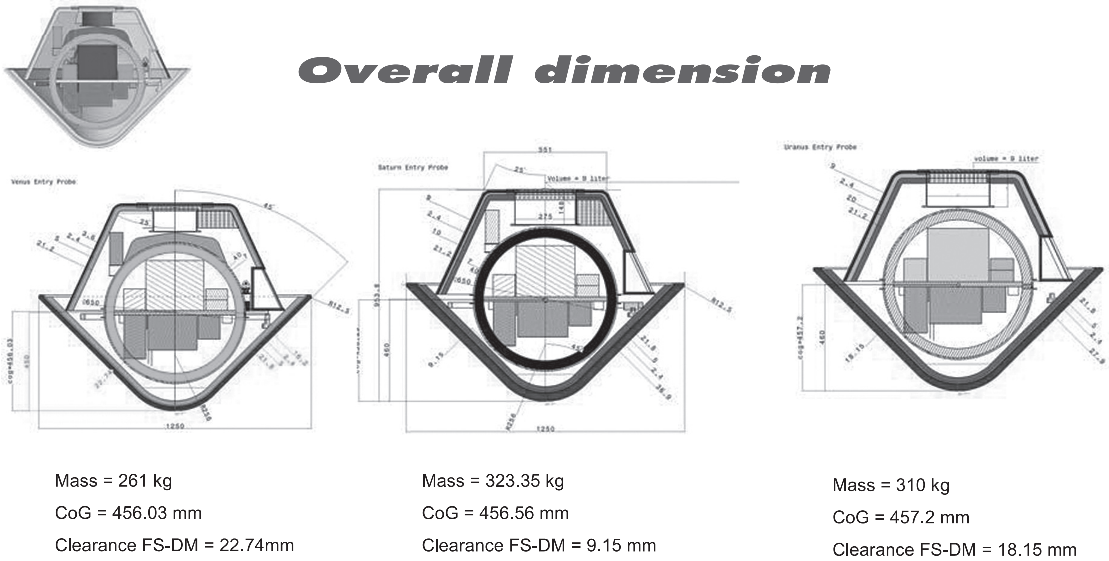

Figure 14.3 Typical dimensions of planetary entry probes investigated by ESA, for the exploration of Venus (left), Saturn (middle) and Uranus (right). CoG: Probe *Center Of Gravity*, Measured from tip of conical front shield (FS); Clearance FS-DM: Minimum space between descent module (DM) and FS (adapted from the PEP Assessment Study Presented at ESTEC on 30 June 2010). (A black-and-white version of this figure appears in some formats. For the color version, please refer to the plate section.)

including helium. As with Kronos, the science payload included an ASI, a sensitive mass spectrometer, a nephelometer, a DWE and a net flux radiometer (NFR). The carrier would have carried a science camera to obtain high-resolution images of Saturn and rings during the flyby. Following the Kronos concept, the Hera carrier would have used LILT solar panels while the probe would use batteries. The mission would have been an international collaboration with NASA who would have supplied the TPS and LILT, and perhaps other systems and instruments.

ESA is currently discussing alternative mission designs. These include a more ambitious concept than Hera to fly a carrier with two probes into the Saturn system, possibly as a large-class mission with budget of ~1 billion euros. One probe would explore Saturn's atmosphere while the other would investigate the composition of Titan's atmosphere and/or that of the geysers of Enceladus. An alternative possibility would be to send a carrier containing several similarly equipped probes to Saturn, Uranus and Neptune that would enable comparisons between the gas and icy giants. However, such a mission would require radioisotope thermoelectric generators, a technology that is not yet sufficiently mature within ESA.

14.3.3 Science Opportunities from Ancillary Saturn Missions

Other opportunities for Saturn science could arise from spacecraft targeted to Saturn's moons Enceladus and Titan, missions supported by the 2016 New Frontiers Announcement of Opportunity. If selected, a Saturn system mission would likely be launched by the mid-2020s. On such a mission, remote sensing cameras and spectrometers, magnetometers and plasma-sensing instruments could provide remarkable new observations of Saturn for several weeks/months on approach to these moons, perhaps for much longer if these missions allow for either satellite or Saturn orbit.

Valuable Saturn science could also be achieved by any appropriately equipped flyby spacecraft that use a Saturn gravity assist. This includes the Decadal Committee's Flagship class Uranus Orbiter and Probe (UOP) mission (NRC 2011) and possible future missions to Neptune and Pluto. Such a mission could provide months of useful flyby observations of Saturn. For Uranus missions, appropriate Saturn GA launch windows of 4–5 years duration occur every 45 years. Voyager 2 utilized the last opportunity when it flew past Saturn in August 1981, encountering Uranus less than 4.5 years later in January 1986. The center of the next opportunity for a Saturn gravity assist occurs in 2026, improbably near to mount a new Uranus mission. The subsequent opportunity for a Saturn kick to the ice giant occurs in 2071.

14.4 Future Observations by Ground-Based and Near-Earth Observatories

With no plans to fund missions to the Saturn System by any of the world's space agencies, ground-based and near-Earth space observatories will likely provide the only certain observations for decades to come. Premier facilities include the large, multi-meter aperture telescopes presently operational and under development in South America and Hawaii, the NASA Hubble Space Telescope, expected to be operational until 2020, and the HST-follow-on facility – the James Webb Space Telescope (JWST) that is currently slated for launch in October, 2018. The JWST is the most complex and most sensitive space-based visual-infrared astronomical telescope developed to date – encompassing a 6.5-meter aperture telescope operating at temperatures less than 50 K – and will be placed at the second Lagrange point (L_2) in a solar orbit some 1.5 million km outside of the Earth, fixed on the Sun-Earth-JWST line, thus ensuring the telescope's high sensitivity by shielding it from both the visible and thermal radiation produced by the Sun, Earth, and Moon, all of which will be on the same side of the spacecraft.

Observations from JWST and large ground-based facilities promise to provide fundamental new information on key Saturn processes, especially as pertains to the planet's response to temporally varying solar inputs. The daily average solar flux at any Saturn latitude varies due to (1) the ~11-year solar cycle that modulates the solar ultraviolet flux and (2) the seasonal variability over Saturn's 29.5-year orbital period produced by both Saturn's orbital eccentricity of 0.054 (resulting in a solar insolation variation of 24% between perihelion and aphelion) and the planet's obliquity of 26.7° degrees (vs 23.4° for Earth and 3.1° for Jupiter). As well, observations from much smaller and less complex ground-based telescopes – particularly those provided by amateur astronomers – promise to provide key information, particularly on the onset and early development of large storms and cometary impacts, as has proven valuable during the past decade (cf. Section 14.5).

14.4.1 Outstanding Science Issues Addressable by Ground-Based and Near-Earth Observatories

14.4.1.1 Long-Term Variability of the Stratosphere and Upper Troposphere

The long-term variability of phenomena in Saturn's stratosphere and upper troposphere typically manifest themselves in meridional variations of temperatures, chemical make-up and winds over latitude (cf. Chapter 10 by Fletcher et al.), as well as more locally in the formation and dissipation of storms and vortices, such as the Great Storm of 2010–2011 (cf. Chapter 13 by Sánchez-Lavega et al.). All such phenomena ultimately provide information on two fundamental issues: (1) "What is the association of the phenomena with seasonal and solar-cycle-induced changes of insolation?", and (2) "what extent is the atmosphere inherently hemispherically asymmetric in its properties?" Resolution of these issues requires observations well past the Cassini time frame.

For over a decade, Cassini has been observing the seasonal variability of Saturn's haze/cloud reflectivity, chemical make-up and temperature. In particular, Cassini/CIRS has been measuring the rate of change of temperature structure and composition over latitude, showing in the short term (several years) favorable comparisons with radiative climate models (Fletcher et al. 2010; and Chapter 10). However, over the longer, decadal term, amounting to about one-third of a Saturn year, these measurements have proven somewhat inconsistent with theory (e.g. Guerlet et al. 2014). Only data gathered throughout Saturn's orbit will provide sufficient coverage to determine the primary sources of heating, including otherwise difficult-to-model radiative absorptions from aerosols. This is particularly the case if the relevant particulates themselves form from seasonally dependent chemistry or are products of phase changes involving seasonally dependent temperature differences.

Other seasonal effects are expected, but have not been documented sufficiently, including the formation of polar vortices, such as the broad, warm polar vortex discovered in an already formed state in the south (Orton and Yanamandra-Fisher 2005) and in the north (Fletcher et al. 2008) that are likely to be the combined result of seasonal warming with boundaries that are governed by dynamical interactions. Any differences

. https://doi.org/10.1017/9781316227220.014

between the evolution of the north and south pole vortices could provide clues to fundamental differences in the internal structure between the hemispheres. The low-latitude oscillation of temperatures discovered in limb sensing by Cassini/CIRS (Fouchet et al., 2008) appeared to be the manifestation of a semi-annual oscillation (SAO; Orton et al. 2008). However, more recent observations noted deviations from that behavior (Sinclair et al. 2014). It remains to be seen whether these departures happen to be the result of the Great Storm of 2010–2011 (cf. Sánchez-Lavega et al. 2012 and Chapter 13) and represent a minor perturbation or whether they are a major phase change of an otherwise stable long-term cycle.

The storm itself and similar precursors (e.g. Sánchez-Lavega et al., 1991) represent unknown time-dependent phenomena whose origins and forcing are still largely uncertain but nevertheless have been the subject of intriguing hypotheses that can be tested over time. In particular, pseudo-cyclical release of latent heat energy from atmospheric water at depth near 20 bar has been recently proposed as the source of power for such eruptions (Li and Ingersoll 2015; cf. Chapter 13), with major eruptions predicted at "storm alley" latitudes (e.g. near the equator, or at mid-latitudes) about every 60 Earth years. As well, the nature and variability of key storm characteristics such as the strength and durability of long-term perturbations of cloud properties or the formation, strength and lifetime of a stratospheric vortex (Fletcher et al., 2012), both so well displayed by the Great Storm of 2010–2011, need to be explored to determine whether such phenomena are similar in all such storms or whether they are different for storms of different strengths.

14.4.1.2 The Variability of Saturn's Auroral Activity with the Solar and Seasonal Cycles

Saturn's aurorae are known to vary partly as a function of solar wind dynamic pressure (Clarke et al. 2009). Therefore, as the solar wind changes over the 11-year solar cycle, Saturn's auroral activity should vary as well. By the end of its 13-year orbital reconnaissance of Saturn in September, 2017, the Cassini Orbiter will have covered an entire solar cycle, obtaining an observational record of myriad solar-induced processes, including auroral processes. However, mixed with the solar cycle is Saturn's 29-year seasonal cycle, which continually changes the geometry of the magnetosphere with respect to the solar wind, likely resulting in a seasonal dependency of auroral activity. This convolution of the length of each season with the period of the solar cycle produces a complex interplay of dependencies that can only be untangled by long-term monitoring of auroral activity. Ground-based infrared observations of H_3^+ emission and space-based ultraviolet observations of H and H_2 emission over several decades would be key components of such a monitoring campaign.

14.4.1.3 Understanding Ring Rain

As detailed in Chapter 8 by Moore et al., the influx of ring-associated water into Saturn was inferred from the presence of dark bands on the planet observed by the Voyager 2 visible camera (Connerney 1986). These dark bands magnetically mapped to features in the rings, indicating that ionized molecules of water from the rings move along magnetic field lines into the planet, chemically altering the makeup of the planet's atmosphere. Using a medium resolution near-infrared spectrograph on the Keck telescope, O'Donoghue et al. (2013) observed this mechanism on a global scale within the ionosphere, revealing an intricate pattern of H_3^+ emissions across the entire northern hemisphere, with a nearly identical companion pattern present at southern magnetic latitudes. Since the magnetic field lines at low latitudes intersect the ring-plane, this strongly suggested that the ionosphere is attenuated by the influx of charged water from the rings. This precipitating water can result in either the net destruction or net production of H_3^+, depending on the flux. This can be investigated with sensitive ground-based telescopes – such as the Keck – during the Cassini Grand Finale in 2017, correlating the planet's H_3^+ pattern with the field lines connecting the rings and the atmosphere as observed in situ by the spacecraft flying just several thousand km above the cloud tops over near-equatorial latitudes. Such data should provide new insights into both (1) the atmospheric chemistry induced by ring particles precipitating onto the planet and (2) changes to the radiative balance of the upper atmosphere generated by these precipitating-particle-induced constituents. Post-Cassini, continued ground-based observations will provide information on the temporal variability of ring rain due to solar cycle variability, particularly as potentially caused by large solar storms.

14.4.2 Observations Obtainable over the Next Three Decades from Near-Earth and Ground-Based Observatories

14.4.2.1 The Prospects from Space Observatories

The 2.4-m Hubble Space Telescope is expected to operate until at least 2020 (www.space.com/29206-how-will-hubble-space-telescope-die.html), providing approximately two years of simultaneous operations with JWST. Until the end of Hubble, Saturn and the other outer planets are slated to be observed with WFPC3 annually under HST's Outer Planet Atmospheres Legacy (OPAL) program (www.stsci.edu/hst/phase2-public/13937.pro). With a spatial resolution of better than 0.1″, the globe of Saturn will be covered over two full planetary rotations each year with multi-filtered images between 220 and 1000 nm, providing an annual determination of large-scale changes in Saturn's mean zonal flow that complement previously observed major changes in the zonal wind (Sánchez-Lavega et al. 2003). Individual General Observer (GO) observations will be possible as well with the WPC3 visible camera and other instruments. Accessing spectral regions unavailable to ground-based observatories, the Space Telescope Imaging Spectrograph (STIS) operates in the near-ultraviolet from 165 to 310 nm, the Advanced Camera for Surveys (ACS) operates over the UV-near-IR from 115 to 1100 nm and the Cosmic Origins Spectrograph (COS) operates in the UV-visible from 115 to 320 nm.

However, at best, even the extended HST operations through 2020 supplement Cassini's on-orbit observations for just three years past the end of the Cassini mission, corresponding to only 10% of a Saturn year. Post-HST, there are currently no plans for UV-visible observations from a funded space-based observatory, although a planetary-dedicated space telescope was proposed to the 2013–2022 Planetary Decadal Survey (Wong et al. 2009). As well, the Large Ultraviolet/Optical/Infrared Surveyor (LUVIOR) 8–16-m-diameter space telescope is currently one of four space-based concepts under study by the National Research Council for the 2020 Astrophysics Decadal Survey (Thronson et al. 2016).

At longer wavelengths, JWST will achieve unprecedentedly sharp Saturn images from near-Earth space when it begins operations in 2018. JWST instrumentation includes the NIRCam near-infrared camera that acquires filtered images from 1.4 to 4.8 μm and includes highly diagnostic spectral regions blocked to ground-based telescopes by telluric absorption, such as the 2.7–3.0-μm region that effectively characterizes ammonia- and water-based condensate hazes and clouds (e.g. Sromovsky et al. 2013). The NIRSpec 1–5 μm spectrometer has a choice of slit widths of 0.1 or 3.3 arcsec and offers an integral field unit (IFU) option with both imaging and spectroscopic capabilities covering a 3×3 arcsec^2 area. Resolving powers of ~1000 or 2700 can be selected (where the resolving power is defined as the observed wavelength, λ, divided by the width of the resolution element, i.e. $\lambda/\Delta\lambda$). At longer wavelengths, MIRI can image Saturn in filters centered between 5.6 and 15 μm without saturation. However, because the planet is so bright, images must be acquired with a 7×7 arcsec sub-array field-of-view (FOV), considerably smaller than Saturn's 20-arcsec diameter. Thus, nine pointings are required to image the entire disk with a 3×3 mosaic. For spectroscopy, similar to NIRSpec, an IFU concurrent imaging/spectroscopy mode targets specific planetary regions, such as the north polar vortex and hexagon, equatorial convective cloud regions and localized cyclones and anticyclones. Spatial coverage ranges from 3×4 arcsec^2 at 5 μm to 7.6×7.6 arcsec^2 at 28 μm. Further details of JWST's observational capabilities are presented in Norwood et al. (2016).

In the early years of the twenty-first century, ESA's X-ray Multi-Mirror Mission, known as XMM-Newton, and NASA's Chandra X-ray Observatory observed X-rays from both Saturn and Jupiter. As reviewed by Badman et al. (2015), distinct differences exist in the character of X-rays emitted by these planets. For Jupiter, X-ray emission is associated with auroral emission, with soft X-rays (<2 keV) attributed to charge-exchange processes and hard X-rays (>2 keV) to electron bremsstrahlung origins. By analogy with Jupiter, Saturn should show soft X-ray emission generated from charge-exchange or bremsstrahlung processes,

. https://doi.org/10.1017/9781316227220.014

but thus far no X-ray emissions have been observed apart from solar X-rays reflected by Saturn's atmosphere. A far more sensitive X-ray instrument concept has been developed for the 2028-launched Advanced Telescope for High-Energy Astrophysics (ATHENA), which will use its X–ray Integral Field Unit (X-IFU; Barret et al. 2016) to conduct a thorough search for Saturn's auroral emissions.

14.4.2.2 The Next 30 Years: Possible Imaging and Reflection Spectroscopy Observations by Large, Ground-Based Observatories

Although space-based missions offer incredible sensitivity and access to spectral regions inaccessible to ground-based telescopes, nevertheless the short lifetime of such missions – typically less than Saturn's 30-Earth-year orbit – necessitates the use of long-lived ground observatories for the consistent monitoring of Saturn's long-term atmospheric evolution. Currently, there are more than a dozen extremely capable medium-to-large diameter telescopes throughout the world (Figure 14.4). In addition to these extant facilities, the US and ESA are developing three more massive, very large-aperture telescopes: the Thirty Meter Telescope (TMT, 30 m), the Giant Magellan Telescope (GMT, 24.5 m) and the European-Extremely Large Telescope (E-ELT, 39 m). With its baselined adaptive optics systems, the TMT promises to achieve diffraction-limited spatial resolution longward of 1 μm, providing 0.007-arcsec imaging at 1 μm (Figure 14.5) with comparable performances expected from the other new facilities. This is sufficient to image Saturn at better than 100 km resolution, superior to all but the best near-infrared images produced by Cassini/VIMS.

These three new exceptionally powerful telescopes will be equipped with state-of-the-art instruments. The TMT, with first light now delayed beyond the 2022 planned opening due to legal disputes over construction on sacred ground at Mauna Kea, Hawaii, plans to support a number of advanced instruments including (1) the Wide Field Optical Spectrometer (0.3–1.0 μm) with imaging and spectroscopy covering a 40-square-arcmin field-of-view (Pazder et al. 2006), (2) the Infrared Imaging Spectrometer (0.8–2.5 μm) that achieves diffraction-limited imaging integral field spectroscopy (Larkin et al. 2016) and (3) the Infrared Multi-Object spectrometer (0.8–2.5 μm) that acquires near-diffraction-limited imaging and spectroscopy over a 2-arcmin diameter field-of-view (Eikenberry et al. 2006). The GMT, with first light planned for 2020, will offer (1) the Visible Echelle Spectrograph (0.35–0.95 μm) with spectral resolving power from 25,000 to 120,000, well suited for precision radial velocity observations (Szentgyorgyi et al. 2014), (2) the Visible Multi-Object Spectrograph (0.35–1.1 μm) with 9 × 9 arc-minute field of view obtained at moderate-spectral resolution (DePoy et al. 2012), (3) the Near-IR IFU and AO imager (0.9–2.5 μm) with 8- to 50-milliarcsec spatial scales feeding an R = 5000 spectrograph (McGregor et al. 2012) and (4) the GMT Near-IR spectrometer (1.2–5 μm) echelle spectrograph that will deliver high R = 50,000–100,000 spectra over five (JHKLM) atmospheric windows in a single observation (Lee et al. 2010).

The E-ELT, with first light planned in the early 2020s, plans as well to have two first-light instruments. MICADO, the Multi-AO Imaging Camera for Deep Observations (Davies et al. 2016), has two imaging modes: (1) a 20-arcsec spatial coverage mode with fine pixel sampling and (2) a 1-arcmin field-of-view mode that maintains diffraction-limited imaging in H- and K-bands. HARMONI, the High Angular Resolution Monolithic Optical and Near-Infrared field spectrograph (Thatte et al. 2014) achieves spectral resolving powers of 500 to 20,000 between 0.47 and 2.45 μm over field of views of 6.42 × 9.12, 3.04 × 4.28, 1.52 × 2.14 and 0.61 × 0.86 arcsec^2. Additionally, a third instrument under construction is METIS, the Mid-Infrared E-ELT Imager and Spectrograph (Brandl et al., 2014). Over 3 to 19 μm, METIS will offer imaging, coronography and medium-resolution spectroscopy over the entire spectral region and high-resolution integral field spectroscopy over 3–5 μm.

For existing 8-to-10-meter-class facilities, improved instrumentation along with improvements in adaptive optics correction techniques promise to make these telescopes even more productive and more sensitive. One such instrument, MUSE, the Multi Unit Spectroscopic Explorer (Bacon et al. 2006), has recently come online at the Very Large Telescope (VLT) in Chile. MUSE spans 0.465–0.93 μm and offers either wide-field (1 × 1 arcmin^2, 0.3–0.4-arcsec spatial

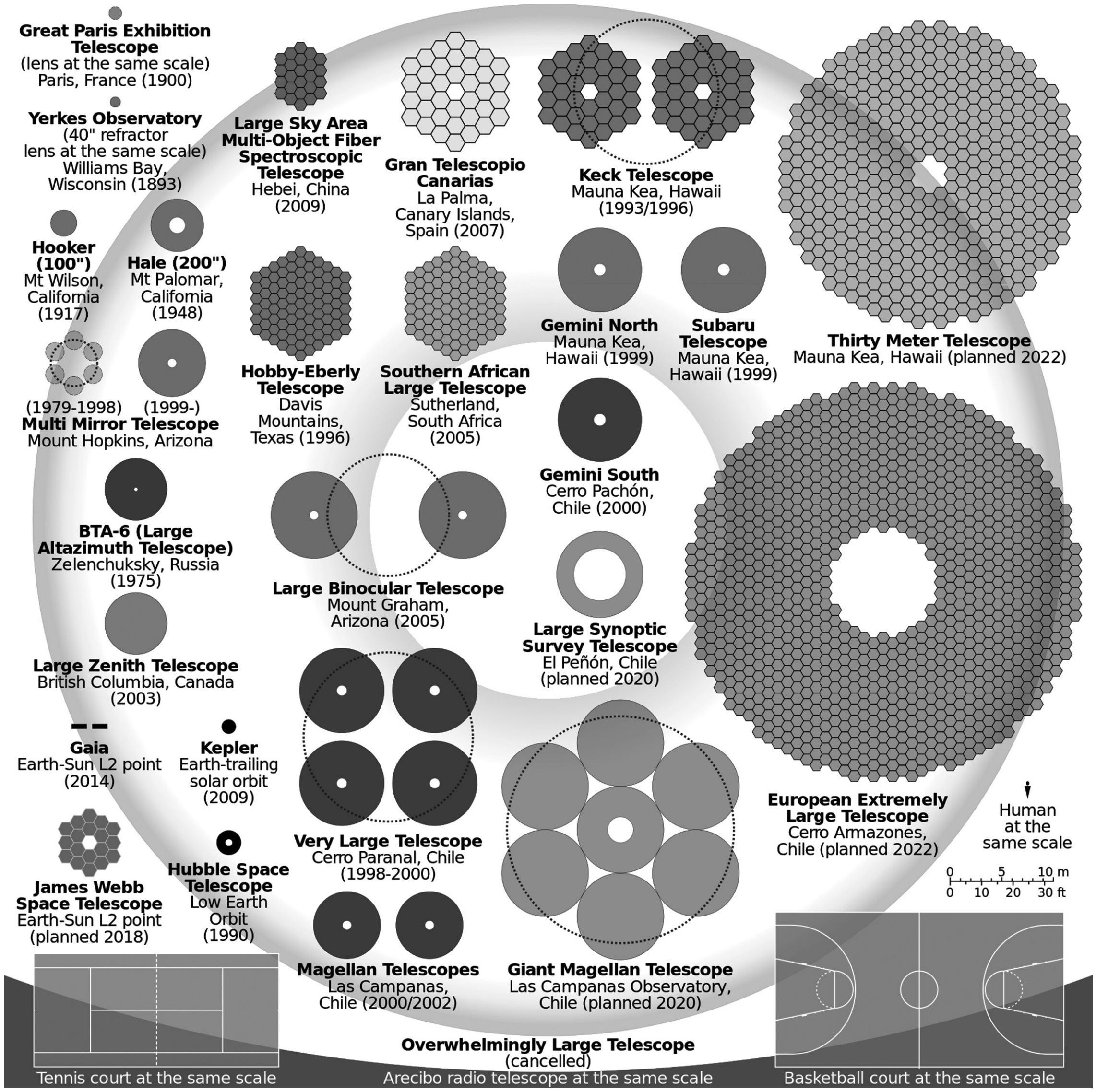

Figure 14.4 Size comparison of the world's largest telescopes. © CMG Lee / http://commons.wikimedia.org/wiki/file:comparison_optical_telescope_primary_mirrors.svg/ CC-BY-SA-3.0 (A black-and-white version of this figure appears in some formats. For the color version, please refer to the plate section.)

resolution) or narrow-field (7.5 × 7.5 arcsec^2, 0.03–0.05-arcsec resolution) integral field spectroscopy at 2000–4000 resolving power. This and other concurrent imaging/spectroscopic instruments are making spectral and spatially resolved observations even more efficient, producing more useful information with less time and overhead.

Although these premier facilities can achieve a vast amount of new Saturn science, the high oversubscription rate from all fields of astronomy will likely significantly restrict their use for studies of Solar System planets. For visible and near-infrared observations, an excellent approach to optimize the time for such in-demand facilities is to use more plentiful, smaller-scale 1- to 3-meter telescopes. Indeed, the ability to perform high-level adaptive optics corrections via laser guide stars is breathing new life into these facilities. One such system, Robo AO (Baranec et al. 2013), can achieve near-diffraction-limited performance in the visible. For example, it is currently possible to achieve 0.1″ spatial resolution in the visible with the Palomar 1.5-meter telescope (Baranec et al. 2014), achieving ~600 km spatial resolution on Saturn at opposition.

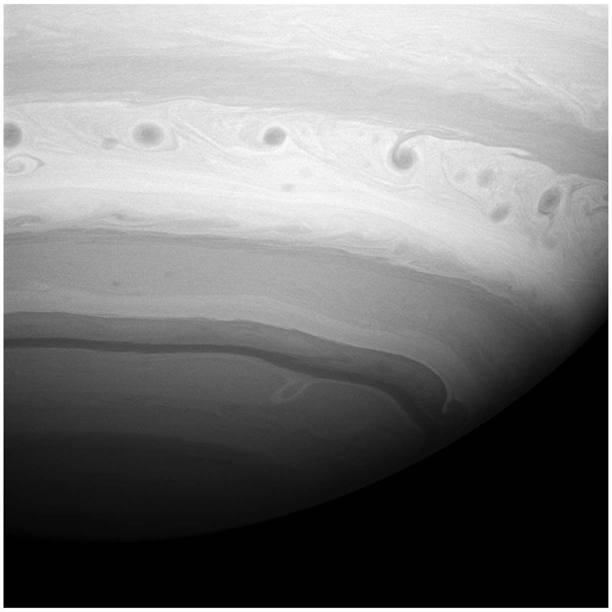

Figure 14.5 Cassini wide-angle camera image of the southern hemisphere Storm Alley in 2008, with a spatial sampling of 48 km/pixel at 728 nm (96 km resolution), comparable to the resolution the TMT will achieve at 1 μm (image courtesy of NASA/JPL-Caltech).

14.4.2.3 The Next 30 Years: Possible Thermal Observations from Large, Ground-Based Observatories

Thermal infrared imaging and high-spectral resolution observations of Saturn can provide detailed insights into the structure and evolution of the atmosphere (e.g. Orton et al. 2008). The mid-infrared allows for the tracking of the temporal evolution of temperatures, photochemical by-products, disequilibrium molecules and clouds. Currently, a number of ground-based instruments are producing valuable mid-infrared observations of Saturn and the other giant planets, including a refurbished MIRSI (Mid-IR Spectrometer and Imager), CELESTE (a high-resolution 5- to 25-μm echelle spectrometer) and HIPWAC (the Heterodyne Instrument for Planetary Wind and Composition) at the 3-m NASA IRTF. TEXES, the Texas Echelon cross-dispersed Echelle Spectrograph, operating at both the IRTF (Greathouse et al. 2005, 2006) and Gemini North, offers both long-slit spectral-scan mapping of Saturn at R = 4,000 and 15,000 as well as high-spectral-resolution scan mapping at R = 50,000–100,000, depending on wavelength. VISIR at ESA's 8-meter VLT is a mid-infrared imager and spectrograph that achieves spectral resolving powers of 150–30,000. Additionally, COMICS, the Cooled Mid-Infrared Camera and Spectrometer mounted on the 8-m Subaru telescope on Mauna Kea in Hawaii, is capable of imaging and spectral measurements with resolving powers of 250–8500 (e.g. Fletcher et al. 2009b). Although no thermal instruments are currently under development for the large 30-meter-aperture telescopes discussed in Section 14.4.2.2, several such instruments are currently planned to be built as second-generation instruments, such as MICHI for the TMT (Packham et al. 2012) and METIS for the E-ELT (Brandl et al. 2014). These could be used, for example, to study the evolution of the stratospheric polar vortex (see Chapter 12 by Sayanagi et al.) in great detail, achieving spatial resolutions of 0.12 arcsec, or ~800 km on Saturn, at 14 μm and 0.24 arcsec, or ~1600 km on Saturn, at 28 μm, for a 30-meter, diffraction-limited telescope.

Submillimeter through millimeter observations of Saturn at high spectral and spatial resolution can be achieved with the Atacama Large Millimeter Array (ALMA). Lellouch (2008), outlining possible very high spectral- and spatial-resolution spectroscopy observations of planetary atmospheres, noted the potential for resolving the 3-dimensional distribution of several species on Saturn and the other giant planets. Determining the vertical profile and meridional distribution of CO in Saturn would provide important clues to the origin of external water and therefor oxygen precipitating into the planet. As well, determining the D:H ratio of high-altitude H_2O will also enable the distinction between its origin from a distance via comets or locally from the ring system. The distribution of stratospheric winds can be mapped in particular at equatorial latitudes, possibly providing evidence of waves perhaps associated with the semi-annual oscillation (Fouchet et al. 2008; Orton et al. 2008).

Spatially resolved microwave measurements can also be made using the Karl G. Jansky Very Large Array (VLA) to measure the distribution of ammonia gas deep in Saturn's troposphere, similar to the mapping of Jupiter by de Pater et al. (2016). Unlike Jupiter, Saturn does not emit synchrotron radiation that could be confused with thermal emission from the neutral atmosphere. Thus, in principal, one could potentially explore the NH_3 distribution deeper than the ~8-bar level of the Jupiter VLA measurements.

Straddling the line between orbital and ground-based observing platforms, SOFIA, the Stratospheric Observatory for Infrared Astronomy (Temi et al. 2014), is a 2.5-m telescope mounted within a 747 aircraft which flies at ~45,000 feet to make observations above most of the Earth's water vapor. EXES, a near twin to the ground-based TEXES instrument, can be used to measure trace Saturn constituents such as H_2O and CH_3, that are currently impossible to measure from the ground due to their low abundance and telluric interference (DeWitt et al. 2014).

14.4.2.4 The Next 30 Years: Auroral Observations

After Cassini, Earth-based observations will once again become the primary means to observe Saturn's aurorae. For nearly three decades, the Earth-orbiting Hubble Space Telescope (HST) has been acquiring crucial ultraviolet observations of Saturn's aurorae. Unfortunately, such space-based observations will end with the demise of HST. JWST will have exceptional spatial resolution and spectral sensitivity in the near-infrared to observe highly diagnostic H_3^+ auroral emissions.

Ground-based infrared telescopes have been observing Saturn auroral H_3^+ emissions since the early nineties (Geballe et al. 1993). Instrumentation on existing facilities include imagers and high-spectral-resolution spectrographs that have provided observations highly complementary to Cassini's measurements. At Mauna Kea Observatory, these include the ISHELL infrared spectrometer and the SpeX medium-resolution near-infrared spectrometer at the NASA Infrared Telescope Facility (IRTF), the NIRSPEC high-spectral-resolution spectrograph at the Keck II telescope and the GNIRS near-infrared spectrometer at the Gemini North telescope. In Cerro Paranal, Chile, the CRIRES high-resolution near-infrared spectrograph is available on the Very Large Telescope. As well, the development of new or updated instrumentation, such as the updated CRIRES on VLT, will provide significant improvements in the quality of auroral observations.

Auroral observations will benefit as well from the development of the three extremely large and adaptive-optics-equipped telescopes described in Section 14.4.2.2, i.e. the TMT, the E-ELT and the GMT. Each of these telescopes will collect over ten times more light than the largest telescope available today. This, in combination with their Adaptive Optics systems, will enable very detailed, high-cadence views of auroral processes. Of particular importance is the detailed characterization of mid-to-low latitude "Ring Rain" (see Chapter 8 by Moore et al.), which utilizes H_3^+ emissions that are very weak compared to the main auroral emissions, requiring the sensitivity of these new instruments.

14.5 Ground-based Amateur Astronomy: Prospective Contributions

The army of experienced amateur astronomers spread across the world is a key asset for the future exploration of Venus. Utilizing commercially available modern yet inexpensive telescopes, computers and software, these volunteer observers regularly produce planetary images that rival those achieved by professional astronomers in spatial clarity and detail, enabling them to periodically make profound discoveries. Indeed, amateur astronomers discovered two of the most dramatic recent phenomena on Jupiter and Saturn: debris clouds produced by an asteroidal collision with Jupiter in 2009 (Sánchez-Lavega et al. 2010) and the breakout of Saturn's Great Storm of 2010–2011, one of the most powerful storms ever witnessed (Sánchez-Lavega et al. 2011; cf. Chapter 13 by Sánchez-Lavega et al. and Figure 14.6).

The major technical advance responsible for such progress has been the development of Video Astronomy. By recording many thousands of short-exposure video frames and then combining only those that show the clearest detail as obtained in moments of the best seeing, amateur astronomers have effectively created a "poor man's adaptive optics" technique. This method uses sophisticated, low-noise video cameras incorporating very sensitive CMOS or CCD sensors, combined with modern, high-quality optics, filters and software to produce high-resolution images that push the level of detail close to the theoretical aperture-determined limit on nights of good seeing, effectively removing much of the detrimental blurring caused by the Earth's atmosphere.

14.5.1 The Development of Video Astronomy

Prior to the advent of affordable, high-sensitivity video cameras suitable for planetary imaging, amateur

. https://doi.org/10.1017/9781316227220.014

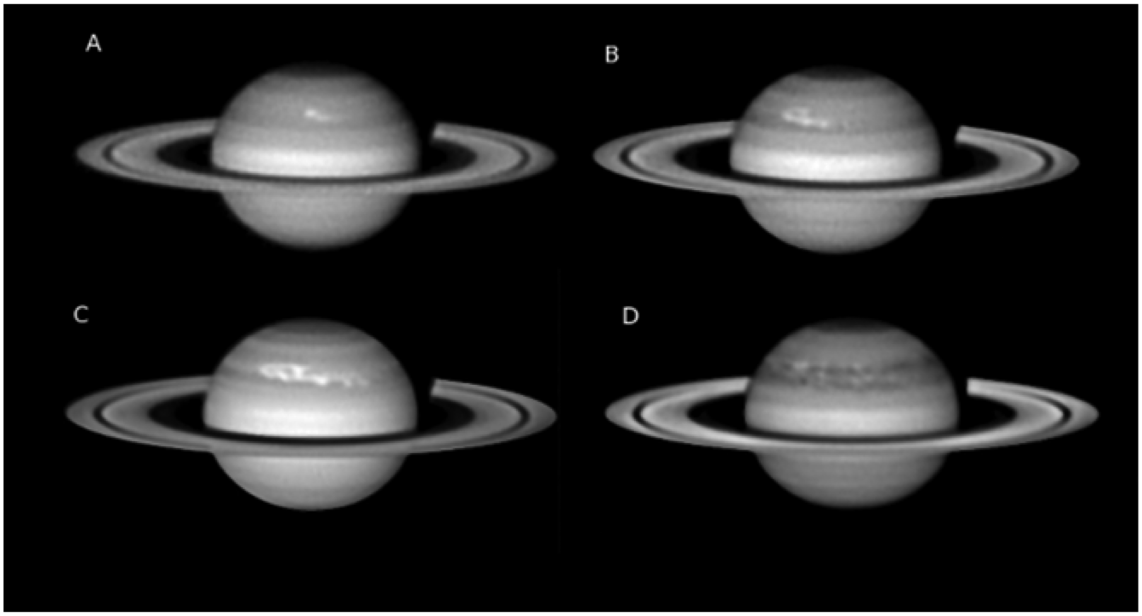

Figure 14.6 Amateur astronomer views of the evolution of the 2010/11Great Storm. A: 14 December 2010, B: 22 December 2010, C: 30 December 2010, D: 2 March 2011 (images © Copyright 2010–2011 by Anthony Wesley).

astronomers typically captured single images with ~0.5-sec exposures, which regularly resulted in blurred images caused by atmospheric turbulence and image motion from local wind-induced tracking errors. In addition, the slow several-second-per-image downloading speed then available limited the number of individual images that could be captured in a single session.

The acquisition of clear, highly resolved images was also hampered by focus drift. In practice, for an F/4 instrument, focus errors as small as 20 microns result in visible image degradation in good seeing. In the 1990s, a large fraction of available observing time was required to obtain and maintain the necessary focus due primarily to (1) flexure in the equipment during tracking, and (2) temperature changes that caused instrument expansion/contraction and thus changes in the optical path.

The late 1990s saw the development of a new breed of low-light-sensitive video cameras for use in internet video conferencing. With transfer rates of 1.1 Mbit/s, corresponding to about 5 frames per second, these video cameras were adopted by the amateur community for relatively rapid planetary imaging. The popular Philips ToUcam camera combined a Sony color CCD (ICX098 BQ) and a lightweight case that could easily be adapted for the modest telescopes in use by amateur astronomers. This sensitive camera spanned 640 × 480 pixels, allowing a usable image scale of ~6 pixels per arc second when operated on a 250-mm-diameter telescope, yielding images of Saturn spanning 70–100 pixels across at the equator. To double the spatial sampling/resolution, a grey-scale version of the ICX098BL detector was used to replace the color RGB Bayer matrix color-sensor (wherein multiple pixels are used to cover the red, green and blue colors necessary to produce a color image; Bayer 1976). A discrete-filter wheel was then typically added to the optical system to obtain images in various colors, including those somewhat beyond the normal visible range.

The advantages of the modern Video Astronomy technique, still used today with much more capable cameras (see Section 14.5.2) include

– Continuous viewing of the target, enabling more accurate, time-efficient and regular focus and camera gain and shutter checks;
– Real-time monitoring of the seeing with improved decision-making on when to record;
– Capturing of thousands of images in a video sequence spanning several minutes, together with efficient automatic editing to find, preserve and combine the best frames.

During the late 1990s, a new breed of free software became available to analyze and reduce the video stream to a final processed image that was greatly superior to anything previously achievable. In particular, the Registax and AutoStakkert software, created by Cor Berrevorts and Emil Kraaikamp, respectively, both of The Netherlands, allowed (1) the re-ordering of the available video frames from best to worst image quality as determined by a user-chosen metric and (2) registration of the chosen best images to a common frame registration using image morphing and inter-frame multipoint alignment techniques to correct for spatial distortions in the individual frames. Combining results obtained in individual color channels enabled the creation of detailed color images.

14.5.2 Recent Advances in Camera Technology

Significant progress has recently occurred in enhanced sensor capabilities, in more sophisticated onboard processing capabilities, and in miniaturization. Today the most powerful commercially available cameras are no more than 50 mm on a side, weigh less than 0.1 kg, and are capable of transmitting up to 5 Gbit, or 100 frames, per second.

The 2010s have seen the maturation of CMOS sensor technology, thus enabling observations at exceptionally low light levels. Currently in early 2017, the 2064 × 1544 pixel Sony IMX252 is perhaps the most advanced sensor, incorporating significant improvements in noise floor reduction and in increased video readout and transmission speed, thus allowing a reduction in shutter speed. This assists in "freezing" the seeing and reducing image distortion in individual frames while maintaining a usable signal-to-noise ratio. For Saturn, a rate of 50 frames/sec is currently achievable, resulting in two-minute sequences of 6000 raw frames per color channel that can be combined into a final image.

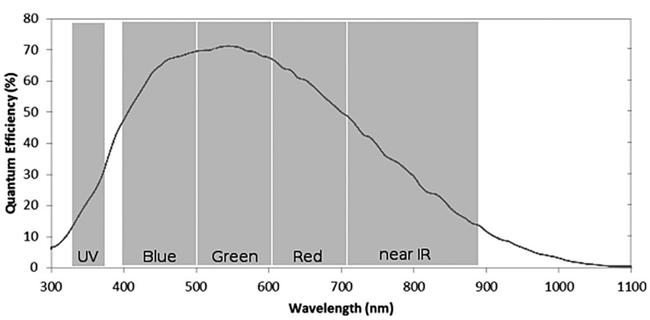

Figure 14.7 Typical response curve for sensors used in modern video astronomy, with the wavelength ranges of typical color filters depicted. Overall, the response is 10% or greater between 330 nm and 900 nm.

The current (early 2017) video astronomy cameras are based on CCD or CMOS silicon sensors with response curves similar to that shown in Figure 14.7. High-quality filters are available in both the 31.7 mm and 51 mm sizes from several vendors, including Astronomik of Germany and Astrodon in the United States.

14.5.3 Contributions of Amateurs to Saturn Science During the Cassini Mission

The eruption of the 2010/2011 Great Storm on Saturn (cf. Figure 14.6) doubled the number of Saturn observations sent to the Association of Lunar and Planetary Observers (ALPO), with 1489 images contributed in 2010/2011. Amateurs followed the storm's formation and evolution, from the first discovery images captured by amateur astronomers Sadegh Ghomizadeh and Teruaki Kumamori on 8 and 9 December 2010 until the storm eventually disappeared during the summer of 2011. It is notable that when the storm erupted, Cassini was not routinely observing the planet, leaving Ghomizadeh and Kumamori to capture the first images of one of the most powerful storms ever observed on any planet.

Continuing to the present day (2017), a compact dark storm remnant has remained visible in the latitudinal region occupied by the storm, as shown in panels B and C of Figure 13.10 in Chapter 13 by Sánchez-Lavega et al. Figure 14.8 shows the location and movement of this feature, revealed by Cassini to be an anticyclonic vortex (cf. Chapter 13), over five years from 2011 to 2016, as predominantly supplied by the amateur community. As well, as shown in Figure 14.9, amateur observers have captured transient dark spots in the rings (so-called "spokes") in good seeing.

In late 2012, as northern summer increasingly tilted the pole toward the Sun and Earth, and aided by an apparent color change, the North Polar Hexagon became visible to amateur astronomers for the first time. The previously uniform dark blue coloration of the north polar region began to change (Image A in Figure 14.10), with the exterior "collar" to the hexagon undergoing rapid changes in visible light. By March 2013 this external collar had changed to a light green,

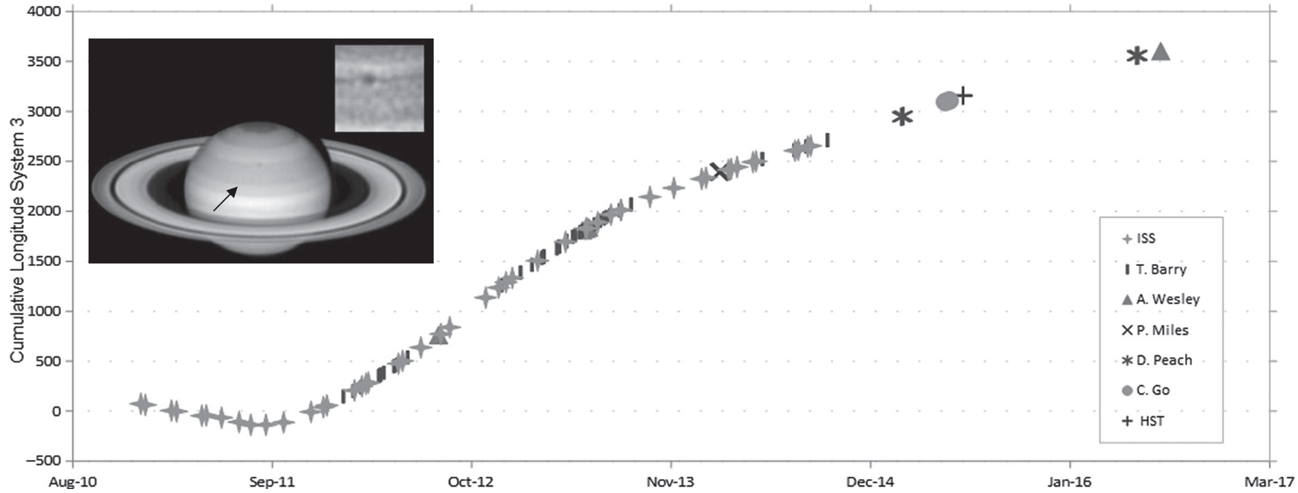

Figure 14.8 Observations of the longitudinal drift of a long-lived compact anti-cyclone on Saturn, 2011–2016, as obtained by five ground-based amateur observers (Trevor Barry, Chris Go, Phil Miles, Damian Peach and Anthony Wesley), the Hubble Space Telescope (HST), and Cassini/ISS (adapted from Sayanagi et al. 2013). Inset shows the feature as observed 18 March 2013 in a red filter image (cf. Figure 14.7) obtained by Anthony Wesley. HST point based on observations made with the NASA/ESA Hubble Space Telescope, obtained from the data archive at the Space Telescope Science Institute. STScI is operated by the Association of Universities for Research in Astronomy, Inc. under NASA contract NAS 5–26555. Graph Credit: Trevor Barry.

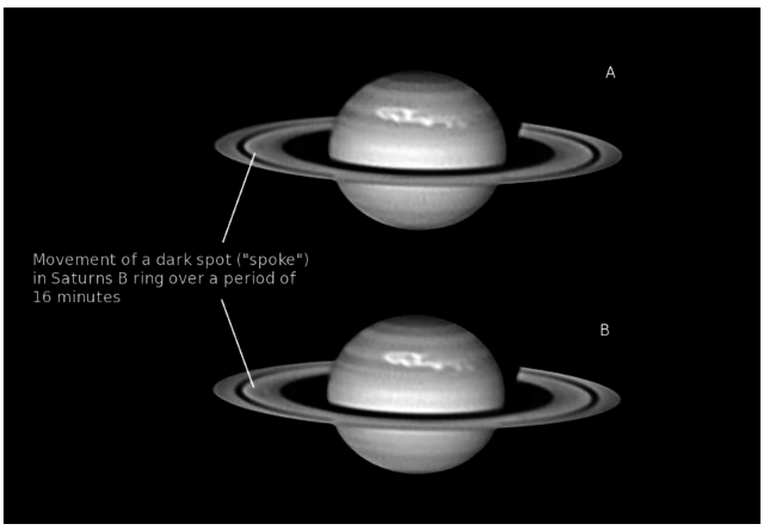

Figure 14.9 Amateur images showing a dark spot ("spoke") in Saturn's B ring. A: 30 December 2010, 1833UTC, B: 1849UTC. Images © Copyright 2010 by Anthony Wesley.

which contrasted with the continuing dark blue interior to render the edges of the hexagon readily visible to amateurs (Image B in Figure 14.10). A short time later – June 2013 – the color of this external collar had changed to yellow (Image C in Figure 14.10), and by April 2014 the color was a distinct red (Image D in Figure 14.10). Throughout, the dark blue interior of the hexagon remained unchanged.

14.5.4 After Cassini: Prospects for 2018 and Beyond

With the demise of the Cassini Orbiter in September, 2017, it will largely be up to the amateur astronomical community to continue monitoring Saturn for the onset of significant phenomena such as great storms, seasonal color changes, and dark ring spokes. In 2018, a

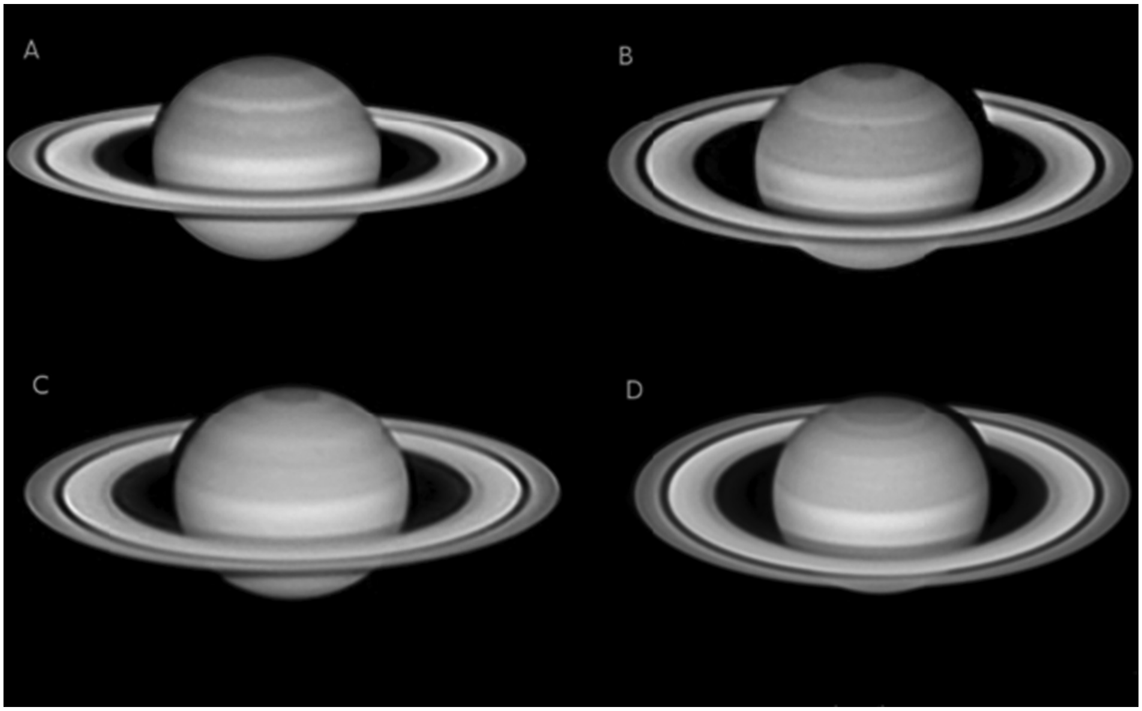

Figure 14.10 Saturn's North Polar Hexagon and color changes 2012–2014. A: March 2012, B: March 2013, C: June 2013, D: April 2014. All images © Copyright 2012–2014 by Anthony Wesley. (A black-and-white version of this figure appears in some formats. For the color version, please refer to the plate section.)

novel astronomical alignment involving Saturn as well as two other bright, photogenic planets occurs as Saturn, Jupiter and Mars appear close together during the perihelic Mars opposition, likely producing enhanced interest in observing Saturn and helping to build an additional army of Saturn observers for many years to come.

14.6 Conclusion

Despite the lack of a funded Cassini–Huygens-style Flagship mission, there is a solid basis for expecting that the exploration of Saturn will continue, with major discoveries being made via both (near) earth-based remote-sensing techniques and small probes that may sample the planet as early as the next decade. In particular, the forthcoming completion of large-aperture, state-of-the-art astronomical facilities on several continents and in near-Earth space (i.e. the James Webb Space Telescope slated for launch in 2018) will undoubtedly provide invaluable new observations on the planet's seasonal and dynamical variability and the workings of its aurorae and major storm systems. The growing army of amateur astronomers, using their own state-of-the-art telescopic equipment teamed with modern digital imaging analysis techniques, will provide an invaluable record of visual images of Saturn of near Hubble Space Telescope quality in spatial clarity, if not in photometric quality, thus alerting professional astronomers to novel new phenomena. Thus, the prospects look bright for effectively addressing many of the prime outstanding issues discussed earlier in this chapter as well as those promulgated by the other thirteen chapters of this book as we witness the continued scientific exploration of the Saturn in the twenty-first century.

References

Aharonson, O., A. G. Hayes, P. O. Hayne et al. (2014), Titan's surface geology. Pages 63–101 in: I. Müller-Wodarg, C. A. Griffith, E. Lellouch and T. E. Cravens (eds.), *Titan: Interior, Surface, Atmosphere, and Space Environment*. Cambridge: Cambridge University Press, Pp.

Atkinson, D. H., J. B. Pollack, A. Seiff (1998), The Galileo probe Doppler Wind Experiment: Measurement of the deep zonal winds on Jupiter. *J. Geophys. Res*. 103, 22911–22928.

Bacon, R., S.-V. Bauer, R. Böhm et al. (2006), Probing unexplored territories with MUSE: A second-generation instrument for VLT. *The Messenger* 124, 5–10.

Badman, S., G. Branduardi-Raymont, M. Galand et al. (2016), Auroral processes at the giant planets: Energy, deposition, emission mechanisms, morphology and spectra. *Space Sci. Rev.* 185, 99–179. doi : 10.1007/s/11214–014-0042–x.

Baranec, C., R. Riddle, N. M. Law et al. (2013), Bringing the visible universe into focus with Robo-AO. *J. Visualized Experiments* 72, e50021.

Baranec, C., R. Riddle, N. M. Law et al. (2014), High-efficiency autonomous laser adaptive optics. *Astrophys. J. Letts*. 790, L8.

Barret D., T. Lam, J.-W. Den Herder et al. (2016), The Athena X-ray Integral Field Unit (X-IFU). Proc. SPIE 9905 Space Telescopes and Instrumentation 2016: Ultraviolet to Gamma Ray. doi 10.111712.2232432. arXiv: 1608.08105v1 (astro-ph.IM).

Bayer, B. E. (1976), Eastman Kodak Co. US patent 3971065. http:/worldwide.spacenet.com/textdoc?DB=EPOC&IDX=US3971065

Brandl, B. R., M. Feldt, A. Glasse et al. (2014), METIS: The mid-infrared E-ELT imager and spectrograph. *Society of Photo-Optical Instrumentation Engineers (SPIE) Conference Series*, Vol. 9147, pp. 21.

Burton, M. and M. Dougherty (2014), Saturn's internal magnetic field: Expectations for Cassini's upcoming proximal orbits, Fall AGU meeting, 2014.

Clarke, J. T., J. Nichols, J.-C. Gérard et al. (2009), Response of Jupiter's and Saturn's auroral activity to the solar wind. *J. Geophys. Res. (Space Physics)*, 114, A05210, doi:10.1029/2008JA013694.

Colwell, J. E., P. D. Nicholson, M. S. Tiscareno et al. (2009), The structure of Saturn's rings. Pages 375–412 in: M. K. Dougherty, L. W. Esposito and S. M. Krimigis (eds.), *Saturn from Cassini-Huygens*. Springer.

Connerney, J. E. P. (1986), Magnetic connection for Saturn's rings and atmosphere. *Geophys. Res. Lett*., 13, 773–776, doi:10.1029/GL013i008p00773.

Coustenis, A., J.-P. Lebreton, O. Mousis et al. (2014), Possible concepts for an in situ Saturn probe mission. *Lunar and Planetary Science Conference* 45, 1244.

Davies, R., J. Schubert, M. Hartl et al. (2016), MICADO: First light imager for the E-ELT. *Society of Photo-Optical Instrumentation Engineers (SPIE) Conference Series*, Vol. 9908.

de Pater, I., R. J. Sault, B. Butler et al. (2016), Peering through Jupiter's clouds with radio spectral imaging. *Science* 352, 1198–1201.

DePoy, D. L., R. Allen, R. Barkhouser et al. (2012), GMACS: A wide field, multi-object, moderate-resolution, optical spectrograph for the Giant Magellan Telescope. *Ground-based and Airborne Instrumentation for Astronomy* IV, Vol. 8446.

DeWitt, C. N., M. J. Richter, K. R. Kulas et al. (2014), First light with the EXES instrument on SOFIA. *AAS/Division for Planetary Sciences Meeting Abstracts*, Vol. 46.

Doody, D. (2004), Basics of Space Flight, Sep. 2004; available at http://www.jpl.nasa.gov

Eikenberry, S., D. Andersen, R. Guzman et al. (2006), IRMOS: The near-infrared multi-object spectrograph for the TMT. *Society of Photo-Optical Instrumentation Engineers (SPIE) Conference Series*, Vol. 6269.

ESA. (2007), Cosmic Vision Call http://sci.esa.int/cosmic-vision/

ESA. (2010), Internal Study, http://sci.esa.int/sre-fp/47568-pep-assessment-study-internal-final-presentation

Fischer, G., W. S. Kurth, D. A. Gurnett et al. (2011), A giant thunderstorm on Saturn. *Nature*. 475, 75–77.

Fletcher, L. N., R. K. Achterberg, T. K. Greathouse et al. (2010), Seasonal change on Saturn from Cassini/CIRS observations, 2004–2009. *Icarus* 208, 337–352.

Fletcher, L. N., B. E. Hesman, R. K. Achterberg et al. (2012), The origin and evolution of Saturn's 2011–2012 stratospheric vortex. *Icarus* 221, 560–586.

Fletcher, L. N., B. E. Hesman, P. G. J. Irwin et al. (2011), Thermal structure and dynamics of Saturn's northern springtime disturbance. *Science* 332, 1413–1417.

Fletcher. L. N., P. G. J. Irwin, G. O. Orton et al. (2008), Temperature and composition of Saturn's polar hot spots and hexagon. *Science* 319, 79–821.

Fletcher, L. N., G. S. Orton, N. A. Teanby et al. (2009a), Methane and its isotopologues on Saturn from Cassini/CIRS observations. *Icarus* 199, 351–367.

Fletcher, L. N., G. S. Orton, P. Yanamandra-Fisher et al. (2009b), Retrievals of atmospheric variables on the gas giants from ground-based mid-infrared imaging. *Icarus* 200, 154–175.

Fouchet, T., S. Guerlet, D. F. Strobel et al. (2008), An equatorial oscillation in Saturn's middle-atmosphere. 2008. *Nature* 453, 200–202.

Fulchignoni, M., F. Ferri, F. Angrilli et al. (2002), The characterization of Titan's atmospheric physical properties by the Huygens Atmospheric Structure Instrument (HASI). *Space Sci. Rev.*104, 395–431.

Geballe, T. R., M. Jagod, T. Oka (1993), Detection of H_3^+ infrared emission lines in Saturn. *Astrophys. J. Lett*. 408, L109–L112, doi:10.1086/186843.

Greathouse, T., J. Lacy, B. Bézard et al. (2006), The first detection of propane on Saturn. *Icarus* 181, 266–271.

Greathouse, T. K., H. G. Roe, M. J. Richter (2005), Changes in the temperature of Saturn's stratosphere from 2002 to 2004 and direct evidence of a mesopause. 36th Annual Lunar and Planetary Science Conference, League City, Texas.

Griffith, C. A., S. Rafkin, P. Rannou et al. (2014), Storms, cloud, and weather. Pages 190–223 in: I. Müller-Wodarg, C. A. Griffith, E. Lellouch and T. E. Cravens (eds.), *Titan: Interior, Surface, Atmosphere, and Space Environment*. Cambridge: Cambridge University Press.

Guerlet, S., A. Spiga, M. Sylvestre et al. (2014), Global climate modeling of Saturn's atmosphere. Part I: Evaluation of the radiative transfer model. *Icarus* 238, 110–124.

Helled, R. (2011), Constraining Saturn's core properties by a measurement of its moment of inertia: Implications to the *Cassini* Solstice Mission, *Ap.J.Lett*. 735, L16.

Hohmann, W. (1925), *Die Erreichbarkeit der Himmelskörper (The Accessibility of Celestial Bodies)*, München: Verlag Oldenbourg.

Jia, X., M. G. Kivelson (2012), Driving Saturn's magnetospheric periodicities from the upper atmosphere/ionosphere: Magnetotail response to dual sources. *J. Geophys. Res*., *117*, A11219, doi:10.1029/2012JA018183.

Koskinen, T. T., B. R. Sandel, R. V. Yelle et al. (2013), The density and temperature structure near the exobase of Saturn from Cassini UVIS solar occultations. *Icarus* 226, 1318–1330, doi:10.1016/j.icarus.2013.07.037.

Lam, T., D. Landau, N. Strange (2009), Broad search solar electric propulsion trajectories to Saturn with gravity assists, AAS Paper 09–355, Proceedings of the AAS/AIAA Astrodynamics Specialist Conference, August 2009, Pittsburgh, PA.

Larkin, J. E., A. M. Moore, S. A. Wright et al. (2016), The Infrared Imaging Spectrograph (IRIS) for TMT: Instrument overview. *Society of Photo-Optical Instrumentation Engineers (SPIE) Conference Series*, Vol. 9908.

Lecacheux, A. and M. Aubier (1997), Re-visiting Saturnian kilometric radiation with Ulysses/URAP. Page 313 in: H. O. Rucker, S. J. Bauer and A. Lecacheux (eds.), *Planetary Radio Emissions IV.*

Lee, S., I.-S. Yuk, H. Lee et al. (2010), GMTNIRS (Giant Magellan Telescope near-infrared spectrograph): Design concept. *Ground-based and Airborne Instrumentation for Astronomy III*, Vol. 7735.

Lellouch, E. (2008), Planetary atmospheres with ALMA. *Astrophys. Space Sci*. 313, 175–181.

Li, C. and A. P. Ingersoll (2015), Moist convection in hydrogen atmospheres and the frequency of Saturn's giant storms. *Nature GeoSci*. DOI:10.1038/NGE02405.

Marty, B., T. Guillot, A. Coustenis et al. (2009), Kronos: Exploring the depths of Saturn with probes and remote sensing through an international mission. *Exp. Astron*. 23, 947–976.

McGregor, P. J., G. J. Bloxham, R. Boz et al. (2012), GMT Integral-Field Spectrograph (GMTIFS) conceptual design. *Ground-based and Airborne Instrumentation for Astronomy IV*, Vol. 8446.

Mousis, O., D. H. Atkinson, M. Blanc et al. (2016), Hera Saturn Entry Probe Mission. A proposal in response to the ESA call for a medium-size mission opportunity in ESA's science programme for launch in 2029–2030 (M5). Submitted to ESA.

Mousis, O., L. N. Fletcher, J.-P. Lebreton et al. (2014), Scientific rationale of Saturn's in situ exploration. *Planet. and Space Sci*., 104, 29–47.

Müller-Wodarg, I. C. F., L. Moore, M. Galand et al. (2012), Magnetosphere-atmosphere coupling at Saturn. 1: Response of thermosphere and ionosphere to steady state polar forcing. *Icarus* 221, 481–494, doi:10.1016/j.icarus.2012.08.034.

NASA, ESA (2009), *Titan Saturn System Mission (TSSM) NASA/ESA Joint Summary Report*, January 19, 2009.

National Research Council (NRC), Committee on the Planetary Science Decadal Survey (2011), *Vision and Voyages for Planetary Science in the Decade 2013–2022*. Washington, DC: The National Academies Press, http://www.nap.edu/catalog/13117.html

Nichols, J. D., B. Cecconi, J. T. Clarke et al. (2010), Variation of Saturn's UV aurora with SKR phase. *Geophys. Res. Lett*. 37, L15102, doi:10.1029/2010GL044057.

Nicholson, P. D., R. G. Drench, A. S. Bosh (1999), Ring plane crossings and Saturn's pole precession. *Bull. Am. Astron. Soc*. 31, 44.01.

Niemann, H. B., S. K. Atreya, S. J. Bauer et al. (2005), The abundances of constituents of Titan's atmosphere from the GCMS instrument on the Huygens probe. *Nature* 438, 779–784.

Niemann, H. B., S. K. Atreya, G. R. Carignan et al. (1998), The composition of the Jovian atmosphere as determined by the Galileo probe mass spectrometer. *J. Geophys. Res*. 103, 22831–22846.

Norwood, J., J. Moses, L. N. Fletcher et al., (2016), Giant planet observations with the James Webb Space Telescope. doi:10.1088/1538–3873/128/959/018005.

O'Donoghue, J., T. S. Stallard, H. Melin et al. (2013), The domination of Saturn's low- latitude ionosphere by ring "rain." *Nature* 496, 193–195, doi:10.1038/nature12049.

Orton, G. S. and P. A. Yanamandra-Fisher (2005), Saturn's temperature field from high- resolution middle-infrared imaging. *Science* 307, 696–698.

Orton, G. S., P. A. Yanamandra-Fisher, M. Brendan et al. (2008), Semi-annual oscillations in Saturn's low-latitude stratospheric temperatures. *Nature* 453, 196–199.

Packham, C., M. Honda, M. Richter et al. (2012), Key science drivers for MICHI: A mid- IR instrument concept for the TMT. Society of Photo-Optical Instrumentation Engineers (SPIE) Conference Series, Vol. 8446. doi:10.1117/12.924996.

Pazder, J. S., S. Roberts, R. Abraham et al. (2006), WFOS: A wide field optical spectrograph for the Thirty Meter Telescope. *Society of Photo-Optical Instrumentation Engineers (SPIE) Conference Series*, Vol. 6269.

Reh, K. et al. (2009), Titan Saturn System Mission Study Final Report. JPL D–48148.

Sánchez-Lavega, A., F. Colas, J. Lecacheux et al. (1991), The great white spot and disturbances in Saturn's equatorial atmospheres during 1990. *Nature* 353, 397–401.

Sánchez-Lavega, A., T. del Río-Gaztelurrutia, M. Delcroix et al. (2012), Ground-based observations of the long-term evolution and death of Saturn's 2010 Great White Spot. *Icarus* 220, 561–576.

Sánchez-Lavega A., T. del Río-Gaztelurrutia, R. Hueso et al. (2011), Deep winds beneath Saturn's upper clouds from a seasonal long-lived planetary-scale storm. *Nature* 475, 71–74, doi:10.1038/nature10203.

Sánchez-Lavega, A., S. Pérez-Hoyos, J. F. Rjoas et al. (2003), A strong decrease in Saturn's equatorial jet at cloud level. *Nature* 423, 623–625.

Sánchez-Lavega, A., A. Wesley, G. Orton et al. (2010), The impact of a large object with Jupiter in July 2009. *Astrophys. J*. 715, L155–L159.

Sanz-Requena, J. F., S. Pérez-Hoyos, A. Sánchez-Lavega et al. (2012), Cloud structure of Saturn's 2010 storm from ground-based visual imaging. *Icarus* 219, 142–149.

Sayanagi, K. M., U. A. Dyudina, S. P. Ewald et al. (2013), Dynamics of Saturn's great storm of 2010–2011 from Cassini ISS and RPWS. *Icarus* 223, 460–478.

Sinclair, J. A., P. G. J. Irwin, L. N. Fletcher et al. (2014), From Voyager-IRIS to Cassini-CIRS: Interannual variability in Saturn's stratosphere? *Icarus* 233, 281–292.

Smith, C. G. A. (2006), Periodic modulation of gas giant magnetospheres by the neutral upper atmosphere. *Annales Geophysicae* 24, 2709–2717, doi:10.5194/angeo-24-2709–2006.

Southwood, D. J. and S. W. H. Cowley (2014), The origin of Saturn's magnetic periodicities: Northern and southern current systems, *J. Geophys. Res*. (Space Physics) 119, 1563–1571, doi:10.1002/2013JA019632.

Spencer, J. R., A. C. Barr, L. W. Esposito et al. (2009), Enceladius: An active cryovolcanic satellite. Pp. 683–724 in: M. K. Dougherty, L. W. Esposito and S. M. Krimigis (eds), *Saturn from Cassini-Huygens*. Springer.

Sromovsky, L. A., K. H. Baines and P. M. Fry (2013), Saturn's Great Storm of 2010-2011: Evidence for ammonia and water ices from analysis of VIMS spectra. *Icarus* 226, 402–418.

Stallard, T. S., H. Melin, S. Miller et al. (2012), Temperature changes and energy inputs in giant planet atmospheres: what we are learning from H_3^+. *Royal Society of London Philosophical Transactions Series A*, 370, 5213–5224, doi:10.1098/rsta.2012.0028.

Szentgyorgyi, A., J. Bean, B. Bigelow et al. (2014), A preliminary design for the GMT- Consortium Large Earth Finder (G-CLEF). *Ground-based and Airborne Instrumentation for Astronomy V*, Vol. 9147.

Temi, P., P. M. Marcum, E. Young et al. (2014), The SOFIA observatory at the start of routine science operations: Mission capabilities and performance. *The Astrophysical Journal Supplement Series* 212, 24.

Thatte, N. A., F. Clarke, I. Bryson et al. (2014), HARMONI: The first light integral field spectrograph for the E-ELT. *Ground-based and Airborne Instrumentation for Astronomy V*, Vol. 9147.

Thronson, H., A. Mandell, R. S. Polidan et al. (2016), Special section guest editorial: Future large-aperture ultraviolet/optical/infrared space observatory. *J. Astron. Telesc. Instrum. Syst*. 2(4), 041201. doi:10.1117/1JATIS.2.4.041201.

Wong, M. H., M. Ádámkovics, S. K. Atreya et al. (2009), A dedicated space observatory for time-domain solar system science. White Paper submitted to the 2009–2011 Planetary Science Decadal Survey, online at www8.nationalacademies.org/ssbsurvey/DetailFileDisplay.aspx?id=186&parm_type=PSDS (see pp. 208–209 of the 2013–2022 Planetary Decadal Survey).

Zander, F. A. (1964), Problems of flight by jet propulsion: interplanetary flights, original publication 1925. *NASA Technical Translation F-147*.

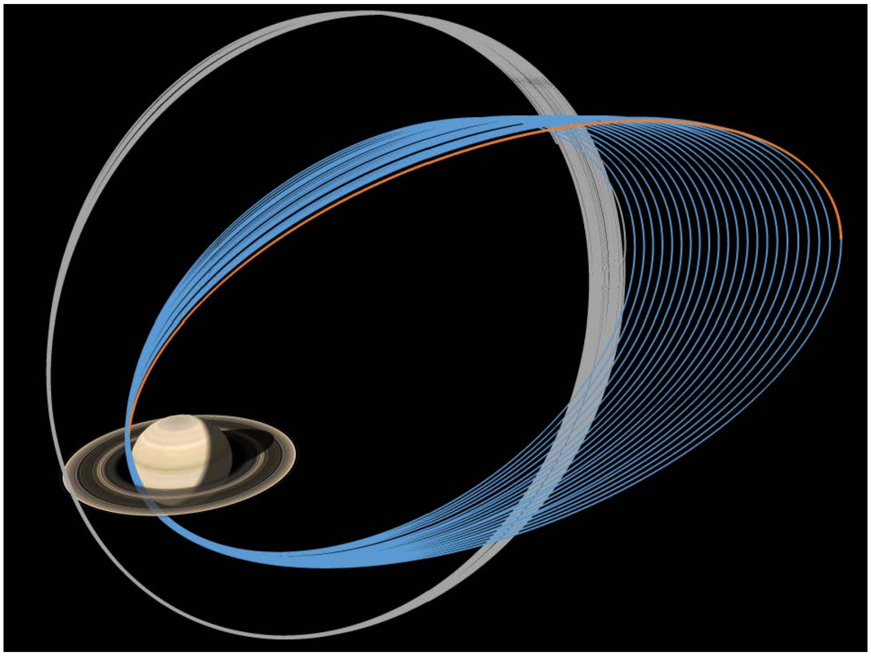

Figure 14.1

Figure 14.2

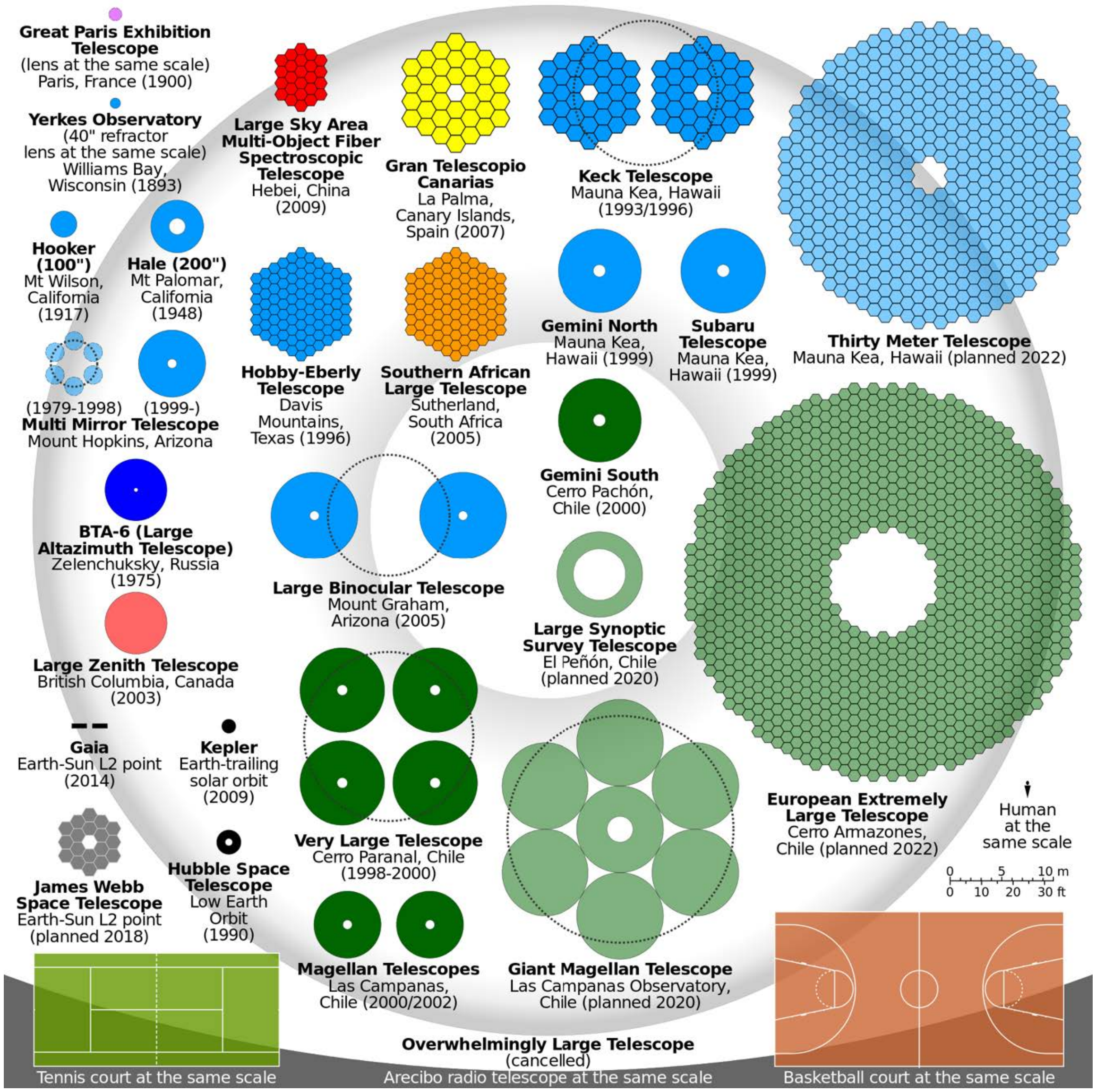

Great Paris Exhibition Telescope
(lens at the same scale)
Paris, France (1900)
Yerkes Observatory
(40" refractor
lens at the same scale)
Williams Bay,
Wisconsin (1893)
Large Sky Area Multi-Object Fiber Spectroscopic Telescope
Hebei, China (2009)
Gran Telescopio Canarias
La Palma, Canary Islands, Spain (2007)
Keck Telescope
Mauna Kea, Hawaii (1993/1996)
Thirty Meter Telescope
Mauna Kea, Hawaii (planned 2022)
Hooker (100")
Mt Wilson, California (1917)
Hale (200")
Mt Palomar, California (1948)
Hobby-Eberly Telescope
Davis Mountains, Texas (1996)
Southern African Large Telescope
Sutherland, South Africa (2005)
Gemini North
Mauna Kea, Hawaii (1999)
Subaru Telescope
Mauna Kea, Hawaii (1999)
(1979-1998) (1999-)
Multi Mirror Telescope
Mount Hopkins, Arizona
Gemini South
Cerro Pachón, Chile (2000)
BTA-6 (Large Altazimuth Telescope)
Zelenchukskу, Russia (1975)
Large Binocular Telescope
Mount Graham, Arizona (2005)
Large Synoptic Survey Telescope
El Peñón, Chile (planned 2020)
Large Zenith Telescope
British Columbia, Canada (2003)
Gaia
Earth-Sun L2 point (2014)
Kepler
Earth-trailing solar orbit (2009)
Very Large Telescope
Cerro Paranal, Chile (1998-2000)
European Extremely Large Telescope
Cerro Armazones, Chile (planned 2022)
Human at the same scale
0 5 10 m
0 10 20 30 ft
James Webb Space Telescope
Earth-Sun L2 point (planned 2018)
Hubble Space Telescope
Low Earth Orbit (1990)
Magellan Telescopes
Las Campanas, Chile (2000/2002)
Giant Magellan Telescope
Las Campanas Observatory, Chile (planned 2020)
Overwhelmingly Large Telescope
(cancelled)
Tennis court at the same scale
Arecibo radio telescope at the same scale
Basketball court at the same scale

Figure 14.4

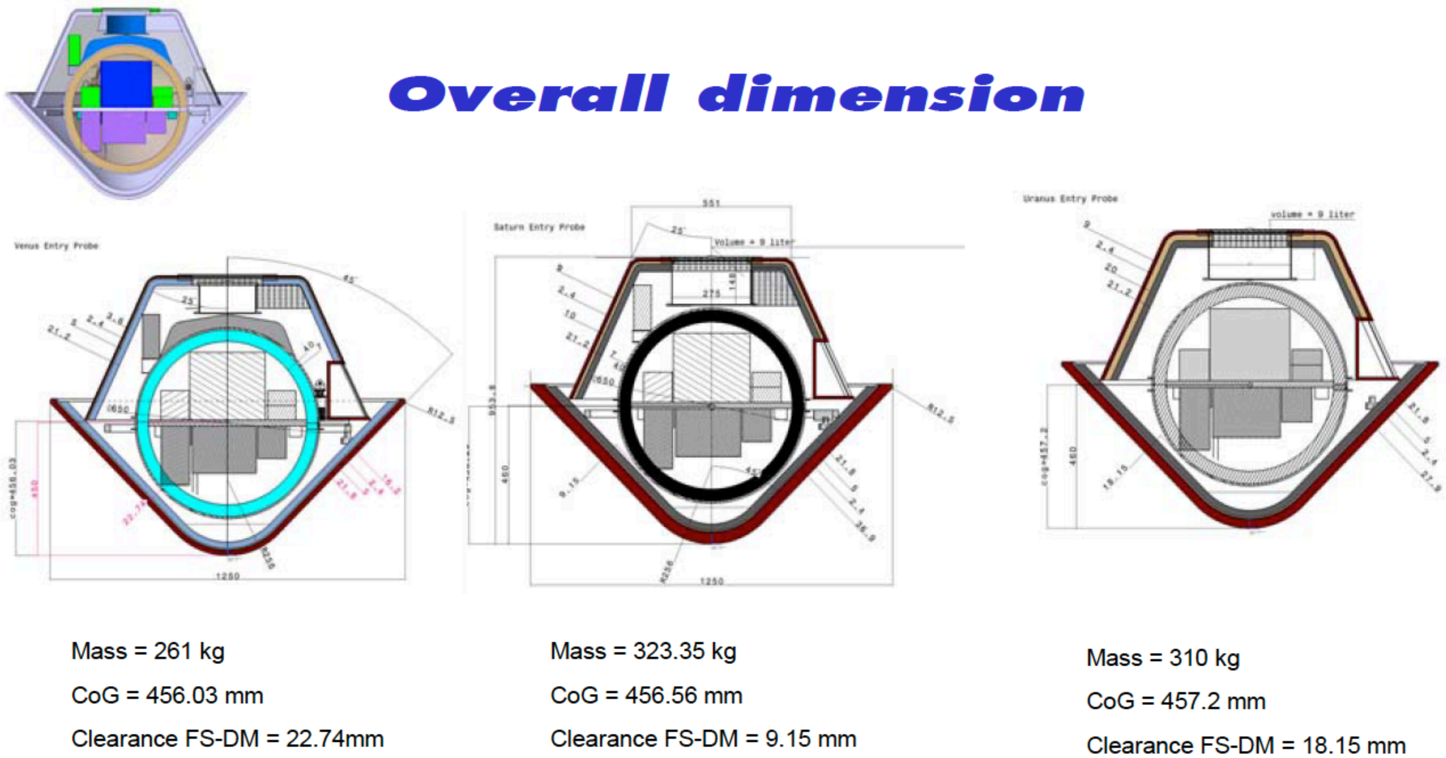

Figure 14.3

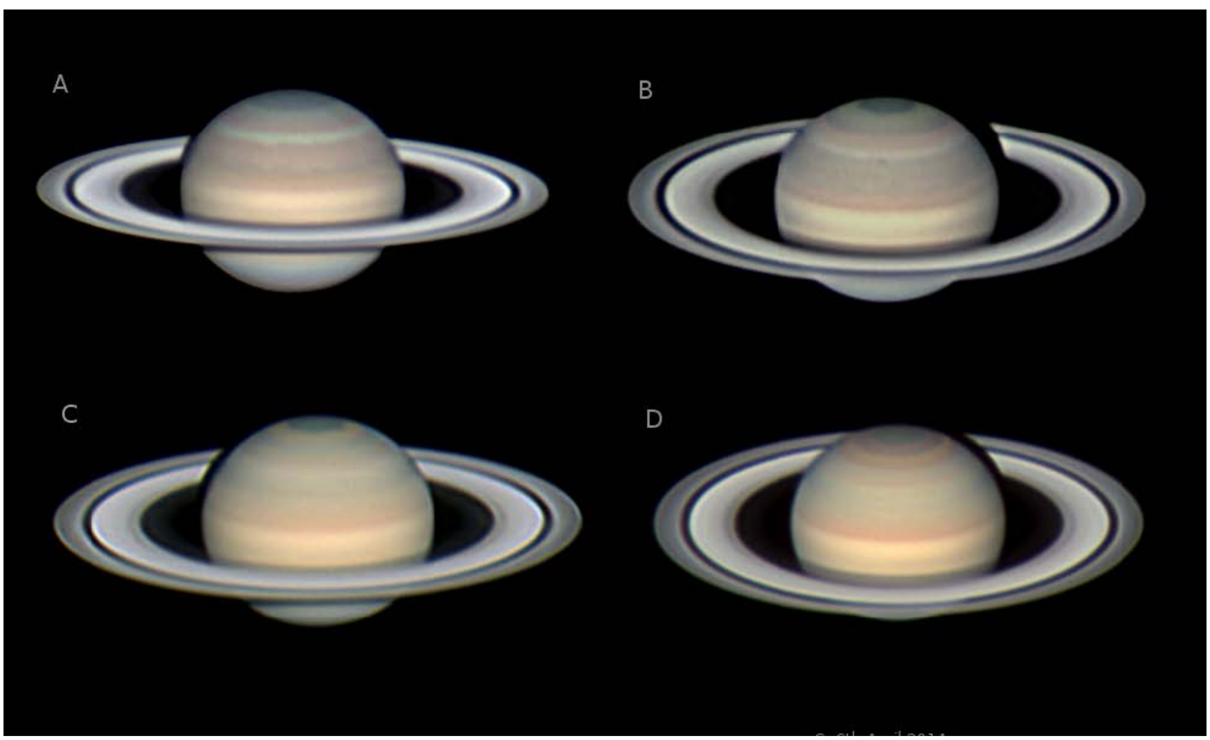

Figure 14.10